ADVANCED ENERGY MATERIALS
www.advenergymat.de

Current Status and Future Perspective on Lithium Metal Anode Production Methods

Begoña Acebedo, Maria C. Morant-Miñana, Elena Gonzalo, Idoia Ruiz de Larramendi, Aitor Villaverde, Jokin Rikarte, and Lorenzo Fallarino**

Lithium metal batteries (LMBs) are one of the most promising energy storage technologies that would overcome the limitations of current Li-ion batteries, based on their low density (0.534 g cm^{-3}), low reduction potential (–3.04 V vs Standard Hydrogen Electrode) as well as their high theoretical capacities (3860 mAh g^{-1} and 2061 mAh cm^{-3}). The overall cell mass and volume would be reduced while both gravimetric and volumetric energy densities would be greatly improved. Their electrochemical performance, however, is hampered by the low efficiency at high current densities and continuous degradation, which are related, among other factors, to the properties of the lithium metal anode (LMA). Hence, the production and processing of LMAs is crucial to obtain the desired properties that would enable LMBs. Here, the conventional method used for the production of LMAs, which is the combination of extraction, electrowinning, extrusion, and rolling processes, is reviewed. Then, the advances in the different alternative methods that can be used to produce and improve the properties of LMAs are described, which are divided into vapor phase, liquid phase, and electrodeposition. Within this last method, the anode-less concept, for which different approaches to the development of advanced current collectors are illustrated, is included.

1. Introduction

The global energy crisis and environmental deterioration have encouraged the development of green energy technologies, which in turn has attracted widespread attention to energy storage devices including lithium-ion batteries (LIBs).[1,2] As the dominant power sources for consumer portable electronics,[3,4] LIBs still cannot fulfill the requirements of other applications such as mobility, for which higher specific energy and energy densities are highly desirable. These properties are determined by the capacity of the electrodes and by the operating voltage. For commercial LIBs, which rely on cobalt-based intercalation cathodes and graphite anodes,[5] the specific energy density could actually overstep 250 Wh kg^{-1}, with a likely growth rate of 7–8% per year.[1–8] Despite the promises to shortly approach the upper theoretical value limit,[6] it would still be far below the desired values for high energy devices, being unable, for instance, to overcome the limits on the driving range of electric vehicles.

In response to this demand, considerable research efforts have been directed toward improving the energy density of LIBs by developing high-capacity cathode materials such as lithium (Li)-rich (or Li-excess) cathodes[9–13] and other high-capacity cathode materials.[14–16] However, the majority of LIBs are still using graphite anodes that, due to the intrinsic limitations of intercalation chemistry, are limiting to high degree the available specific energy density, being a true bottleneck for many applications.

Furthermore, fast charging rates are becoming a key element as well for the development of next-generation batteries, especially to accelerate the widespread use of electric vehicles. However, graphite anodes are unable to achieve fast charging without adversely impacting the battery performance and safety. In fact, when LIBs are charged at high rates, high current densities induce large graphite-anode polarizations resulting in limited energy utilization.[17–20] Moreover, the graphite anode can reach electrochemical potential values lower than the thermodynamic potential of Li metal, making Li plating a favorable process.[21] The formation of metallic Li on graphite anode surface causes irreversible loss of Li, leading to significant cell capacity fading, as well as safety issues.[21–23] Besides, European Union has considered graphite as one of the critical raw materials.[24]

In this respect, some alternative materials, from which silicon (Si) has attracted special attention, have been proposed

B. Acebedo, M. C. Morant-Miñana, E. Gonzalo, A. Villaverde,
J. Rikarte, L. Fallarino
CIC energiGUNE
Basque Research and Technology Alliance (BRTA)
Alava Technology Park, Albert Einstein 48, Vitoria-Gasteiz 01510, Spain
E-mail: jrikarte@cicenergigune.com; lfallarino@cicenergigune.com

B. Acebedo, I. Ruiz de Larramendi
Department of Organic and Inorganic Chemistry
Universidad del País Vasco (UPV/EHU)
P.O. Box 664, Bilbao 48080, Spain

The ORCID identification number(s) for the author(s) of this article can be found under https://doi.org/10.1002/aenm.202203744.

DOI: 10.1002/aenm.202203744

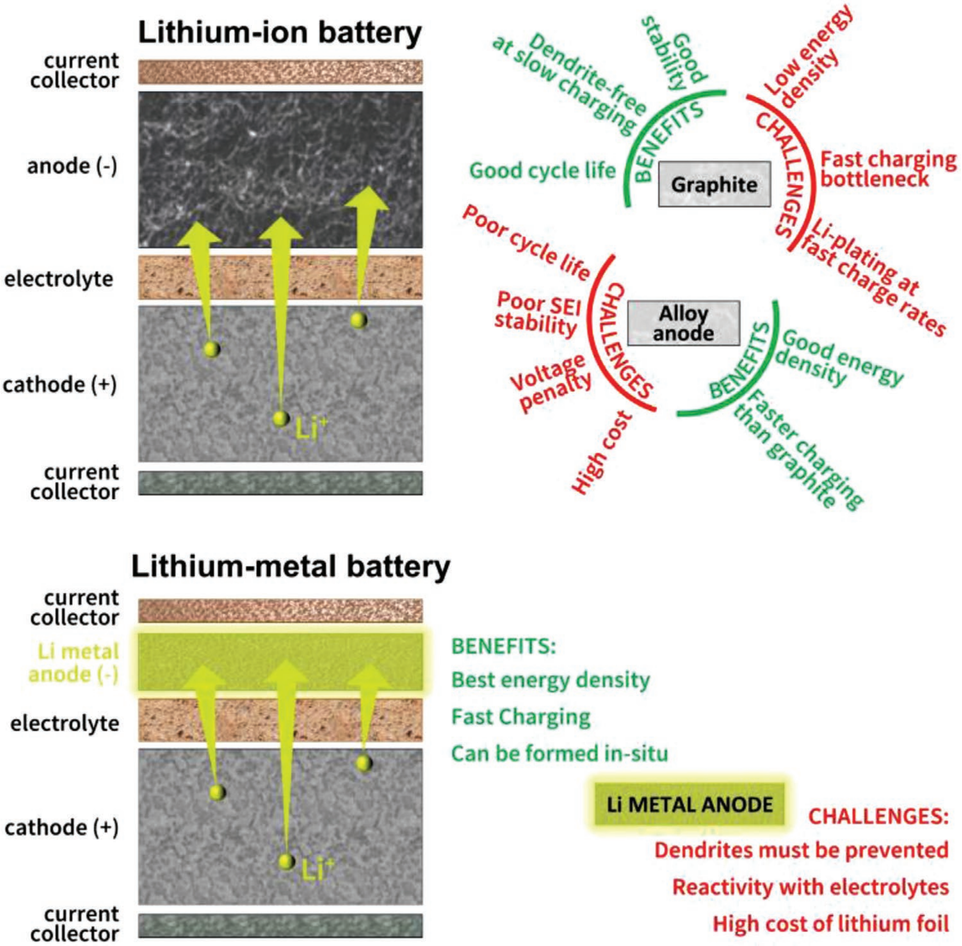

Figure 1. (Left) Schematic comparison between Lithium-ion and Lithium-metal batteries; (right) benefits and challenges of three types of anodes: graphite, alloy-based, and Li-metal.

as candidates to replace graphite in anodes, based on the increased theoretical capacity they offer.[25,26] However, lithium ions do not intercalate neatly; instead, electrochemical alloying reactions take place in these alternative materials, creating an entirely new phase. As a result, all these materials experience a dramatic volume change upon lithiation and delithiation,[27,28] which causes the anodes to crack, to electrically disconnect from the active material, and finally to pulverize over many cycles.[29] Moreover, many alloy anodes have large initial irreversible capacities (the difference between charge and discharge capacity).[30,31] There may be few workarounds for these problems, such as the prelithiation of the anodes, the use of high pressures to prevent cracking, or the use of nanostructured anodes that can accommodate the volume expansion. However, all of them have serious tradeoffs and add high cost while making manufacturing far more difficult. Additionally, Si anodes also suffer from a voltage penalty that reduces cell energy. Alternative compositions with lowered Si-content and a similar working voltage as graphite are under study, e.g., silicon–graphite (SiG) mixtures.[32] Despite reducing both volume change and side reactions, while maintaining a high capacity, effective, and controllable manufacturing technique should be still developed to obtain low electrode swelling, requiring much more efforts for future widespread applications.[32] Therefore, there is an unmet need to go beyond Li-ion technology to simultaneously achieve high-energy density and efficient fast charging.

Concerning the anode side, Li metal is considered as the uttermost material because of its highest theoretical gravimetric capacity of 3860 mAh g^{-1} and the lowest electrochemical potential (−3.04 V vs standard hydrogen electrode),[33] as schematically described in **Figure 1**. Li metal anode (LMA) can be paired with different cathode materials, such as intercalation based (e.g., $LiFePO_4$,[34] $LiNi_xCo_yMn_{1-x-y}O_2$[35,36]) or multielectron conversion chemistry-based cathodes (as in Li–S[37] or $Li–O_2$ batteries[38]), to achieve different levels of energy density and produce different battery technologies according to the specific needs. LMA also plays an important role in the development of solid-state-batteries (SSBs).[39,40] In most cases, the specific energy densities of batteries employing LMA have the potential to reach over 500 Wh kg^{-1}.[41,42]

Nevertheless, rechargeable Li-metal batteries have not yet been to a great extent commercialized. LMA was already applied in rechargeable batteries in 1980s, but safety issues limited their use and have been the major challenges hindering the practical applications since then.[43,44] The main origin of safety issues comes from the formation of Li whiskers and dendrites, which is induced by unstable interfaces between Li metal and the electrolyte. All these remaining problems, in addition to causing security risks, are also related to the low efficiency and poor performance of lithium metal batteries, as stated in recent reviews.[45–47] It is necessary not only to control the deposition of lithium below the interface, but also to avoid continuous side reactions between the LMA and the electrolyte in addition to controlling the infinite volume change during cycling.[48] Many works and reviews have already specifically focused on different strategies toward enabling lithium metal in batteries.[49–54] The challenges concerning LMAs implementation and performance have been, as of now, extensively explored, and its discussion goes beyond the scope of this article.

On the contrary, not so many works have focused on the effect that the fabrication process of LMAs has on their inefficient use in cell performance. In fact, the production of LMAs still encounters many crucial challenges, such as quality, reactivity, handling, safety, etc. Moreover, despite Li is fairly abundant in Earth, the supply needs to be extracted from brines or underground reserves, and current mining operations might not be sufficient to keep up with the industry's growing needs. Additionally, metallic lithium in the form of Li^0 is only achieved by electrowinning of LiCl-KCl and no alternative to this industrial process is expected in the short term. Therefore, novel strategies are needed to reduce the amount of lithium used in LMAs in order to enable it as anode.

Here, we aim to review the state-of-the art on current Li extraction, LMA fabrication and processing methods and introduce alternative strategies that are currently under study. Several fabrication methods are covered, ranging from conventional method based on Li metal obtention, metal extrusion, and rolling to alternative methods here classified as vapor-based, liquid-based, and ex situ and in situ (anode-less) electrodeposition methods. We account for the remarkable progress achieved in each technique by reporting the recent developments and by discussing the research highlights obtained by several groups. Finally, we conclude the review article with an outlook on future challenges. This review aims to be a useful introductory resource for readers from the outside or just starting in this field. It also provides thorough description on the current LMA fabrication processes and potential alternative methods for those who already have an established understanding of the topic; it includes perspectives on the strengths and weaknesses of each method toward commercialization of LMAs with improved properties.

2. Production of Lithium Metal Anodes

As mentioned above, LMA emerges as a potential candidate to replace current graphite anodes used in Li-ion batteries due to its properties. For LMAs to be successfully implemented in LMBs, though, their efficiency upon cycling needs to be improved. The fabrication and processing methods used for the production of LMAs have an impact on their properties, being, thus, a crucial part for the development of high performing LMBs. In this section, standard industrial processes are described, followed by the developments and potential alternatives that could be implemented in the future.

2.1. Industrial Standard Process

2.1.1. Extraction

Metallic Li is highly reactive with ambient components, and, thus, it never occurs freely in nature. Therefore, it needs to be extracted out of lithium compounds that are geographically distributed across the Earth´s crust (**Figure 2**) mainly located in salt pans that exist along the lithium triangle (54% of the world's lithium reserves). Lithium deposits are mainly found in brines or spodumene pegmatites and, to a small extent, in sedimentary rocks.[55] Brines are saline waters with high contents of dissolved salts. They are extracted from aquifers located mainly in Chile, Argentina, China, and Tibet and pumped into shallow evaporation solar ponds for about 2 years to eliminate deleterious elements and compounds, principally magnesium and sulfate.[56] In addition, this evaporation process enriches the brines until 6000 ppm of LiCl, which is then reacted with Na_2CO_3 (soda ash) to yield Li_2CO_3, the most common precursor of lithium metal. Spodumene pegmatites deposits, on the other hand, are coarse-grained intrusive igneous rocks, mainly found in Australia, that were formed from the crystallization of magma at certain depth in the crust. In this case, the Li_2CO_3 is obtained from the concentrated pegmatite ore. The mineral is heated to about 1100 °C to make it more reactive and after grinding and mixing it with hot sulfuric acid, it is heated to 250 °C to form Li_2SO_4. Water is added to dissolve the Li_2SO_4, which is finally treated with soda ash to yield Li_2CO_3. Although the produced lithium concentration is higher, this process is more expensive making it less competitive than other sources such as brines.

In both cases, the obtained Li_2CO_3 material (or the LiOH that can be also obtained) can be directly employed to produce cathodes, although, in order to have metallic lithium, the transformation of the precursors into raw LiCl (anhydrous) is

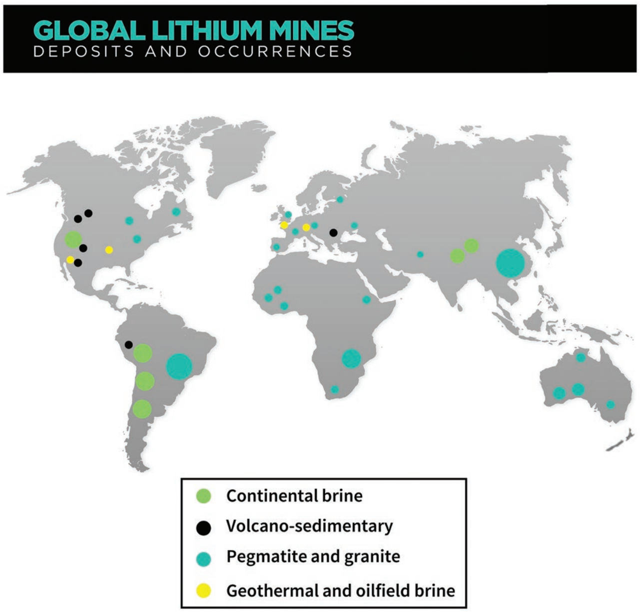

Figure 2. Schematic map of the global lithium mines, deposits, and occurrences. Based on ref. [239].

needed. The production of LiCl involves the reaction of Li_2CO_3 with HCl and subsequent crystallization of LiCl after reaching temperatures close to 100 °C. LiCl must be stored in dry atmospheres to protect it from moisture. As a result, this industry transforms natural resources into basic materials through processes that require high energy inputs being part of the energy-intensive processing (**Figure 3**a).[57] The industrial method was invented about 100 years ago,[58,59] and barely changed ever since. This process, also known as the electrowinning method, electrolyzes the LiCl component of the molten LiCl-KCl eutectic in the temperature range of 450–500 °C.[60,61]

Currently, the methods of producing LiCl-KCl compounds vary from the origin of the feedstock and can be adapted to improve the purity of the final product. The selection of the extracting method of Li from brines is limited by the presence of contaminant multivalent ions (Mg/Li mass ratio), and the effects of other competing coexisting ions, such as Na^+ and K^+. For instance, the application of the evaporation precipitation method is limited to brines with high Mg/Li ratio because the pre-processes needed for removing coexisting ions are highly complex and time-consuming. Therefore, some alternatives, such as column adsorption and diffusion dialysis are employed.[62] These methods employ either Li-selective adsorbents (activated carbon or spinel type materials) or osmotic distillation membranes to achieve a high degree of saturation of LiCl in the aqueous solutions. Additionally, these Li-enriched solutions can by further augmented in Li by ion exchange, sequential adsorption, or solvent extraction. The efficiency of these processes could be enhanced by combining them with electro-membranes since this technology allows for the extraction of lithium in higher grades.[63] From spodumene ores, Li is recovered chemically or through a combination of chemical and pyro-metallurgical processes. Two different processes, namely, roasting and calcination or chlorination and leaching (either in acidic or alkaline aqueous solutions) are reported to recover high purity Li compounds from ores.

The LiCl-KCl eutectic is formed at the temperature of 353 °C with a molar ratio of 59:41. At this temperature, lithium metal is obtained via electroreduction of Li^+ ions on the cathode in the liquid form (Equations (1)–(3)), as the melting point of metallic Li is 180.5 °C[64]

$$\text{Cathode reaction:}\quad Li^+ + e^- \Rightarrow Li \tag{1}$$

$$\text{Anode reaction:}\quad Cl^- + e^- \Rightarrow 1/2Cl_2 \tag{2}$$

$$\text{Net reaction:}\quad LiCl \Rightarrow Li + 1/2Cl_2 \tag{3}$$

Moreover, due to its small density, Li metal floats on the surface of the LiCl-KCl eutectic and facilitates the isolation of the pure metal. Hence, the eutectic phenomenon is greatly desired and beneficial for electrowinning of lithium because it allows to produce metallic lithium at much lower temperatures with a low energy consumption. Unfortunately, the process lacks sustainability due to the high operating temperatures needed and the generation of toxic Cl_2 gas as a byproduct.

Worldwide researchers are trying to overcome these drawbacks by exploring new alternatives based on the modifications of the current industrial method. Most of the strategies are based on the application of electrowinning technology to nonindustrial eutectics or thermal reduction or decomposition via pyrolysis of lithium compounds.[65] Other novel approaches are based on the use of solar-power electrolysis of brines[66] and the extraction of Li from both seawater and salty lake water with the $FePO_4$ electrode using the electrochemical intercalation method.[67] To easily collect the metallic Li, electrochemical extraction of Li from molten LiOH using a liquid tin cathode with a high molar content of Li in the product has been reported.[68] Electrodeposited materials from LiCl dissolved in an amide solvent in the form of thin film were transformed into bulk material by smelting.[69] Using the same approach high pure Li metal films with a controlled morphology and thickness are produced by electrolytic deposition of lithium.[70]

Since the industrial method employs harsh conditions for the electrowinning process, a typical synthesis cell (Figure 3b) must consist of a highly resistant cell body in which a graphite anode and a mild steel cathode are immersed in a fused LiCl-KCl eutectic bath as the electrolyte. In addition, argon gas is purged above the molten salt surface to protect Li and the reactor from oxidation and corrosion. In operation, the newly formed lithium metal wets the surface of the steel cathode, rises to the surface of the bath, and forms a pool of molten metal. Liquid lithium is dipped from the cell with an iron dipper and cooled to about 300 °C to solidify the amount of salt present. The metal is then cast onto iron molds and coated with an industrial, white mineral oil to limit further reaction with the atmosphere.[71] Once the lithium metal ingot is obtained it is extruded to form a film, rolled to reduce the thickness, and passivated to conduct further manufacturing steps and avoid oxidation with the storage.[72] These steps will be individually discussed in the following section.

2.1.2. Extrusion

Extrusion is a metal forming process, widely used in industry, in which a round billet is placed in a chamber and submitted to a force applied by an asymmetric die. In the case of lithium metal extrusion, the force is applied by a hydraulically driven ram and the process is called hydrostatic extrusion (Figure 3c). The use of a fluid avoids the contact between the ram or container and the lithium metal billet. The friction between the billet and the chamber is eliminated due to the plastic deformations that occur because of the high hydrostatic pressure. Thereby, the pressurized fluid acts as a lubricant between the billet and the die.[73] The main factors considered to determine the extrusion pressure are the die angle, the reduction in cross-section, the extrusion speed, and the billet temperature/lubrication.[74] The extruded product can be obtained in the form of bars, rods, strips, or sheets. The strips can be as thin as 250–400 µm with a good surface finishing but poor thickness uniformity. To mitigate these limitations, the ingot can be formed into a thin sheet by adapting the extrusion die with a die holder.[75,76]

2.1.3. Rolling

Depending on the size of the final battery, variations in all the dimensions of the strips are required and thereby the

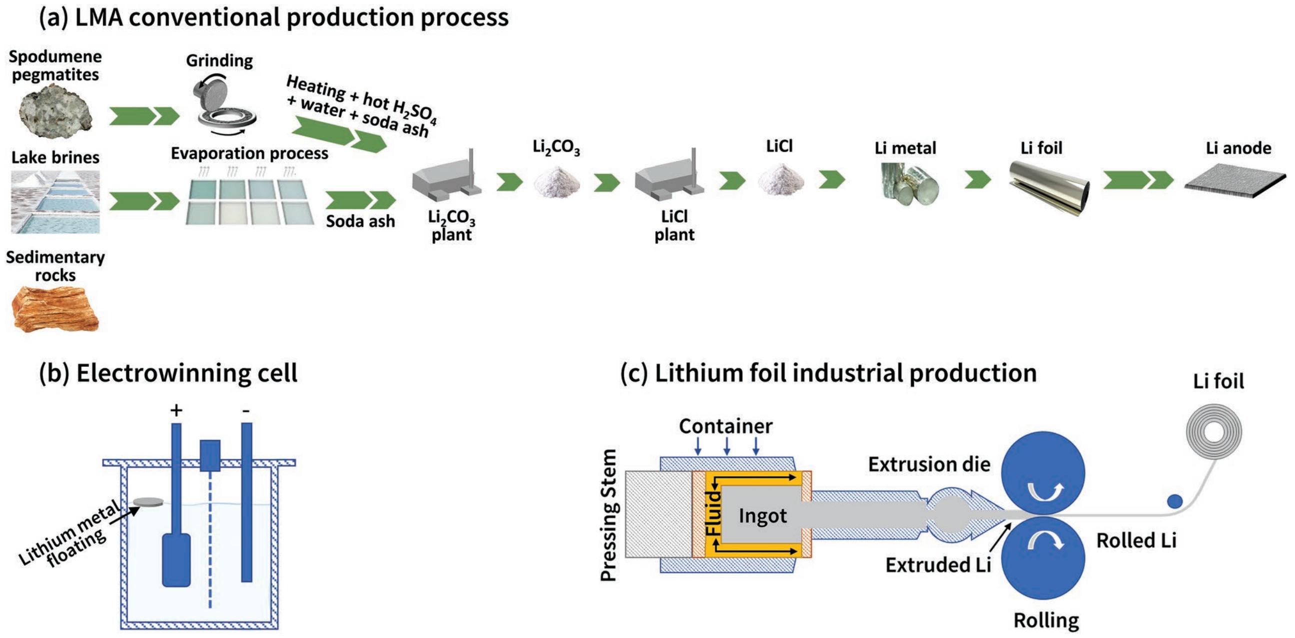

Figure 3. Schematic of: a) conventional lithium metal anode production process; b) electrowinning cell for lab scale; c) lithium metal foil industrial production process.

extruded product must be subjected to external pressure.[77] This process is also known as cold rolling and allows for high throughput production and the adaptability of the extruded product into dimensions of the cell formats. The high-intensity process (line loads greater than 500 N mm^{-1}) for lithium metal differs from conventional calendering of other electrodes since metallic lithium is nonporous, and thickness as low as 10–20 µm are sometimes targeted.[78] The use of polymeric supporting layers covering either the lithium metal or the rollers can facilitate the processing since lithium is very adhesive and the obtention of damage-free thin-films after the rolling step is challenging. This method is used commercially to produce limited quantities of strips of 30–75 µm thick.[79] Some alternatives employ rolling additives as lubricants that make possible control the tension applied to the film and gives lithium of ≈22 µm with relatively good flatness.[80] Similar approaches[81] were employed to continuous production of rolls 30 m long by 15 cm wide. A significative reduction in defects without the use of lubricants has been achieved by adding a gettering material to the molten lithium metal and separating them by filtration.[82] After forming the ingot, the extruding and the rolling the film, the final thickness was ≈20 µm.

Besides obtaining a self-standing lithium foil, the lithium metal can also be combined with planar or perforated metal foil as current collectors to form a negative electrode sheet with reduced weight.[83] The pore size, the thickness of the metal current collector (CC) and the nature of the contact layer are important parameters to improve the binding force of the lithium electrode and prevent the poor electrical contact between both elements. In this regard, strong affinity was generated in a nanostructured lithium metal electrode by calendering and subsequent folding of lithium and lithium tin alloy ($Li_{22}Sn_5$) enabling for stable lithium stripping/plating cycling under ultrahigh current densities.[84]

Tension is also a key component in the rolling process and is usually applied for detaching the film in a controlled manner[85] allowing for films with thickness close to 20 µm. However, this parameter should be minimized in the foils being extruded. Too much tension would induce camber into the extruded foil, as well as negatively affect the surface appearance and internal grain structure of the lithium metal foil.[86]

Compared to the extrusion process, the rolling process is more costly, and the number of rolling steps increases the cost of the process.[87] To minimize this, Stumper et al.[88] studied the effect of the lithium foil geometries, line load, and roller temperature on the deformation behavior of the lithium foil to stablish a semiempirical model to predict the lithium processing and validity ranges. Unfortunately, the densification toward 0% has still not been solved by the industry.

In some cases, a winder is coupled with the roller to wind the lithium directly after the rolling process. This coupling requires a delicate balance between the pressure and tension created by both components and the speed of the winder must exactly match the speed of the extruder, so that the finished foil is not torn or stretched, retaining all the dimensional characteristics required and removing the resulting tensions in the materials. Lithium must be processed in a dry atmosphere, or it will oxidize, when in contact with ambient air, resulting in a poor quality of the product. Therefore, it must be passivated to be used in the subsequent process under dry-room conditions. For passivation, multiple approaches such as gas treatment, coating with a layer of polyethylene wax, or surface fluorination are available. The most common method to remove the passivation layer includes mechanical scraping, roll pressing, and hexane cleaning. For instance, the kerosene on the lithium ingot surface was first removed with an oil-absorbing paper and after that, the lithium ingot surface was scraped with the rough polypropylene. Second, the surface layer was removed with a clean surgical knife and finally it was wrapped with

Polyethylene terephthalate (PET) film and pressed into foils by hydraulic machine.[89]After these treatments, lithium metal is considered clean. However, even if it is stored in the glove box or under ultrahigh vacuum, lithium metal will inevitably react with trace gases, and its surface will be again passivated, which will inhibit further reactions.

The passivation layer can, in addition, act protectively to suppress lithium metal dendrite formation/growth, and to suppress reaction of lithium metal with electrolyte, which would result in a reduced cell performance due to electronic conductivity and/or decompensation. The electrochemical properties of lithium metal are highly dependent on the native and solid electrolyte interphase (SEI) films. This layer is composed of various lithium compounds such as Li_2O, Li_2CO_3, and LiOH, which are commonly formed on lithium metal even in an inert atmosphere. The performance of native and SEI films on lithium metal could be significantly enhanced through appropriate heat treatment during extrusion of the lithium ingot,[90] by flattering the topography of the electrodes by roll-press technique,[91] by modifying the surface of the chemistry of the native layer[92] or by removing it.[93] Other approaches have employed structured (either pillars or pyramids) to force the deposition of the Li alongside these wall structures[94] or have tuned the mechanical methods for the obtention of lithium electrodes with {110} texturing.[95] This preferential orientation is obtained by prerolling and scraping a 600 µm foil and subsequent annealing and rolling the resulting film.

After passivation, the mother coil is laser-slit to daughter coils or single electrodes. Mechanical roll-knife slitting, which is the established process for LIBs, is not suitable, due to the adhesive properties of Li. Lithium metal foils are finally stacked together with polymer,[96,97] gels,[98] and polymer composite[99] electrolytes at lab and industrial level.[100]

Despite being a well stablished industrial process developed for long time, lithium films commercially available do not meet the requirements of quality, length, width, and thicknesses required for the assembly of LMBs at competitive costs. Thus, alternative processing techniques are needed, if beyond Li-ion battery technologies based on LMAs are successfully going to be commercialized. Such alternative techniques under study and their recent developments are discussed in the following sections.

2.2. Vapor-Based Techniques

Physical vapor deposition (PVD) techniques are methods to deposit thin-films and coatings by the transport of material from a condensed matter source, via the gas phase, to another surface to be coated. In contrast to conventional ceramic processing, where materials are heat-treated or densified at high temperatures,[101] PVDs are robust and efficient methods that allow for the preparation of coatings with high reproducibility and high quality at significantly lower temperatures. Moreover, in order to minimize any possible source of process poisoning, ultrahigh vacuum (UHV) conditions are set prior and during any deposition.

The actual deposition process depends on several parameters such as the selected materials and the substrate to be coated, the substrate temperature, the system geometry, and the kinetic aspects of the growth. Except under very special conditions, the deposition usually leads to polycrystalline arrangements consisting of many crystallites or grains with different relative crystallographic orientation. They can be randomly oriented, due to statistical randomness, or they can show preferential orientations, i.e., a crystallographic texture.[102] On the other hand, coatings with specific crystallographic order can be fabricated by epitaxial growth, meaning that the crystallographic order of the deposited layers is induced and controlled by that of the substrate.[102]

PVD techniques are being employed in a widespread range of applications, and they can be regarded as an essential aspect of microelectronics, optics, storage media, hard and corrosion resistant coatings, and many more.[101,102]

Because of their design, PVD has enough versatility to utilize virtually any type of inorganic and some organic coating materials on an equally diverse group of substrates and surfaces, being able to create a wide range of alloys, multilayers, or composite materials. Furthermore, different PVD techniques can be combined to deposit given layers of multilayers coatings.

The deposition rates in PVD-processes are highly dependent on the processing conditions and typically range between 0.1 and 100 nm s^{-1}. Accordingly, this leads to layer thicknesses from a few angstroms (Å) to hundreds of micrometers (µm) with process times varying from fractions of seconds to hours. For solid-state battery research, the most important PVD processes are sputtering, pulsed laser deposition (PLD) and evaporation (thermal and electron beam) techniques. Simplified schematics of each process are shown in **Figure 4**. Sputter deposition and evaporation processes are already well-established in industrial processes due to their ability to coat large areas, including roll-to-roll processes, whereas PLD was limited to small substrate sizes for many years. In the last decade, the available areas for coating increased substantially due to beam widening and shaping, with orders of magnitude higher output powers compared to typical PLD laser systems for research.[103]

Vacuum and energy uptake during the phase transition from the condensed phase to the gas phase are important aspects and are discussed in more detail in the following sections in which the fundamental characteristics of widely applied PVD techniques are described.

2.2.1. E-beam Vapor Deposition

The e-beam vapor deposition (EB-PVD) method is based on the action of an electron beam, which is given off, under UHV, by a tungsten filament that is heated up to the point where thermionic emission of electrons takes place.[104] The generated electron beam is accelerated to a high kinetic energy and steered by means of a magnetic field toward the material target, commonly placed into a crucible. Upon striking the target, the electrons lose their energy very rapidly, with their kinetic energy converted into thermal energy that heats up the target causing it to melt or sublimate, as schematically depicted in Figure 4a. Accordingly, the material is transformed into vapor and coats the surface of the substrate.

The highlighted advantages of EB-PVD are the very low level of impurity of the coated layers, the high deposition rate, the

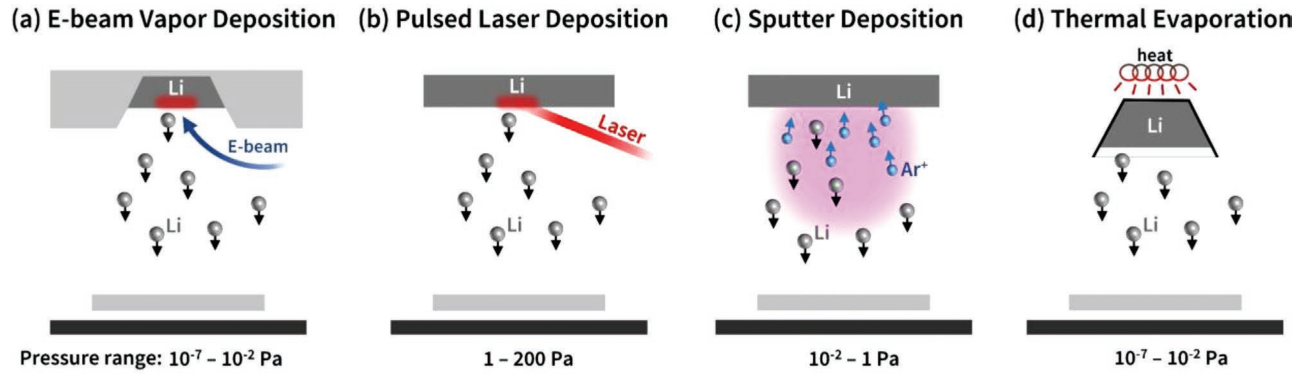

Figure 4. Schematic illustrations of four different PVD techniques employing lithium sources. The small blue spheres represent the Ar^+ ions, whereas the gray ones the lithium leaving the target source.

good directionality of the ejected material from the target, the high material utilization efficiency, while being suitable for metals and dielectrics with high melting points. Moreover, it is compatible with ion-assist sources. EB-PVD can be widely used for optical coatings such as high purity film and conductive glass. It also has potential industrial applications for wear-resistant and thermal barrier coatings in aerospace industries, hard coatings for cutting, and tool industries, due to the strong adhesion between coatings and substrates.[104,105]

However, very few works have shown EB-PVD as a valuable tool to evaporate metallic lithium as anode of a solid-state battery, solely focusing on advancing the understanding of solid–solid (electrolyte/lithium) interfaces.[106,107] Therefore, EB-PVD still need to demonstrate its ability to be a suitable mean for the fabrication of Li-metal anodes.

2.2.2. Pulsed Laser Deposition

PLD evaporates the material through one or a series of high energy laser pulses, as sketched in Figure 4b. The target material to be deposited is placed in a rotating holder inside a stainless-steel chamber where UHV is established prior to any deposition. The substrate, which is also located inside the chamber, can be heated, if necessary, since substrate holders usually include a resistance that allows the temperature to be raised. During PLD processes, a series of complex physical reactions occur, which transform the solid-state material (target) into a vapor phase by interaction with the laser radiation, generating an energetic plasma plume made of atoms, molecules, and ions. The plasma condenses on the surface of the substrate thanks to the particular geometry of the component arrangement inside the chamber, where the laser strikes at an angle of 45° relative to the target surface (Figure 4b).

In order to obtain the correct stoichiometry of the deposited layers, a series of parameters must be controlled. The level and quality of the UHV prior to depositions is one of the critical factors along with the selection of the optimal gas environment, which includes the correct choice of carrier gas and its partial pressure inside the chamber (background gas pressure). For the deposition of oxides, such as layered oxides or perovskites, oxygen is usually used as transport gas,[108] but if the material is sensitive to oxidation in that environment, the use of inert atmospheres such as argon and even argon/hydrogen mixtures are usually chosen.[109] The temperature to which the substrate is heated and the nature of the substrate itself influence the type of growth of the layer, being possible to obtain single-crystal, polycrystalline, or amorphous films. Furthermore, the substrate (lattice parameters, orientation, and temperature) is crucial to produce an epitaxial growth of the thin layer.

The source of the pulsed laser radiation is also very important in the deposition of high-quality thin layers and in the control of the thickness of the films. Among the more important laser parameters there are its characteristics (wavelength, pulse duration, dimension of the beam, or distribution of energy), the laser fluence (generally between 1 and 3 J cm^{-2}), and the repetition rate. Moreover, the deposition time (main film thickness control) and the distance between the target and the substrate are also crucial.[110] By controlling all these parameters, it is possible to obtain thin layers of both pure metals or alloys[111] and more complex systems such as stoichiometric multielement oxides.[112,113]

For battery research, PLD has played and plays an important role in the development of microbatteries. These batteries avoid the use of liquid solvents, being completely solid devices where the entire system has a thickness of few micrometers. In this way, it is possible to deposit by PLD thin layers of each component of the microbattery separately or even to manufacture the device completely by means of this technique through the sequential growth of the different components.[114,115] Another interesting application focuses on the structuring of C-based anodes or current collectors, which enables the stabilization of the lithium-metal anode since lithium nucleation occurs preferentially in the defects that act as nucleation centers.[116–118]

Regarding LMAs, thin lithium layers have been prepared on 2 cm^2 stainless steel (SS) substrates at room temperature using a KrF excimer laser.[119] This work sought to acquire a better understanding of the factors that affect the growth of dendrites throughout the lithium metal stripping/plating processes. To achieve this goal, the authors studied different lithium surface states obtained from different methods: electrochemical treatment, lithium metal polishing and PLD. The latter produces metallic lithium deposits with a homogeneous and rough morphology, showing the presence of particles with a grain size of 400 nm, as can be seen in **Figure 5**, left.[119] No preferential growth is observed, which was expected when using

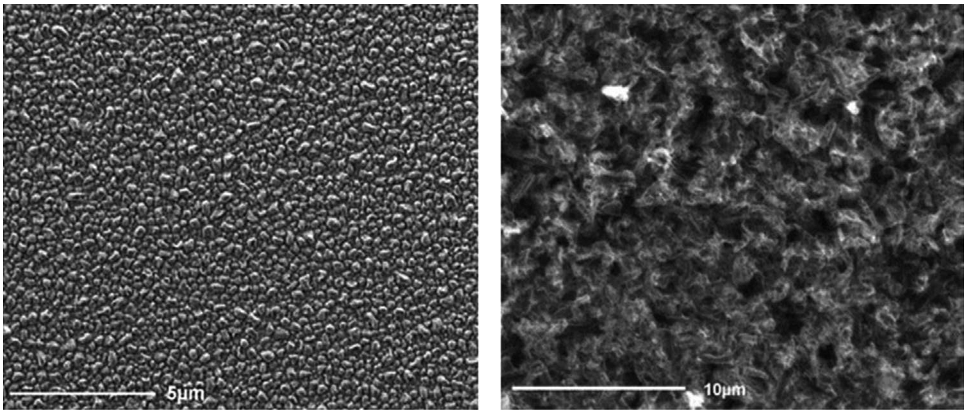

Figure 5. (Left) Surface morphology of lithium thin films prepared by PLD. (Right) Surface morphology after lithium plating on lithium thin-film in EC/DMC–LiPF$_6$ 1 M at 1 mA cm^{-2}. Reproduced with permission.[119] Copyright 2006, Elsevier.

SS substrates. In the study of lithium plating, after applying a polarization of 1 mA cm^{-2} on thin layers of lithium 1 µm thick, rough nondendritic plated lithium morphologies are observed (Figure 5, right).[119] Hence, proving that on smooth and polished surfaces (with less concentration of defects) the current density distribution is more homogeneous, showing less/null dendritic growth.

As far as the authors are aware, there are no other scientific works in which the use of PLD is applied to obtain layers of metallic lithium. Indeed, lithium is extremely reactive to moisture traces, which complicates its handling. The vacuum chamber where the laser ablation will be performed should be equipped with at least a glove box to avoid lithium contamination. This drawback, together with the high cost of the system and the limitation in terms of the area of the thin film that can be obtained, means that PLD might not be the most convenient for working with lithium. However, the Finnish company Pulsedeon, focused on developing next generation Li-ion battery solutions based on PLD technology, markets thin-Li-metal-anodes manufactured using this technique.

In conclusion, although PLD is not the most appropriate for obtaining thin-films of lithium, it can still hold a relevant position for the future of lithium metal batteries or in the development of the next generation of anode-less lithium metal batteries, through the optimization of the surface of the current collectors.

2.2.3. Sputter Deposition

In a basic sputtering process, a target material is bombarded by energetic inert Ar$^+$ ions that are generated by the glow discharge plasma situated in close vicinity of the target material.[120] An electric potential difference is established between the chamber wall and the material target to accelerate the Ar$^+$ ions toward the negatively charged target material to strike it with enough kinetic energy to tear off atoms from it. The extracted atoms move toward an appropriately positioned substrate. A schematic of the process is depicted in Figure 4c, where the small blue spheres represent the Ar$^+$, whereas the gray ones the material leaving the target source.

Generally, the Ar$^+$ flow responsible for the erosion of the target is continuously generated by the plasma itself, with no need of any external ion supplier. The rate of the material leaving the target depends primarily on the number of bombarding Ar$^+$ ions. This can be further increased by placing an array of permanent magnets behind the target to create a static magnetic field, which leads to much higher self-regeneration yields for the plasma and higher deposition rates.[121,122]

The sputtering process is usually generated by a direct current (DC). In the case of nonconductive target materials, an alternating radio frequency (RF) power is instead applied[123,124] to neutralize the positive charging at the target surface. Sputter deposition has multiple advantages, such as fast deposition speed, low rise of substrate temperature, and high purity films with good compactness and uniformity. The sputtering process has very good repeatability, and the film with a uniform thickness can be obtained on a large area substrate.[120,123,124] At the same time, the film's grains and crystallite size can be controlled by changing the sputter parameters, and different metals, alloys, and oxides can be mixed and sputtered on the substrate simultaneously.[125,126,127] Moreover, it is easy to industrialize.[128]

To improve battery performance and fabricate specific batteries, since 1993,[129] magnetron sputtering has played a key role in the growth of thin-film electrode materials,[130–132] solid-state electrolytes,[133–136] separators,[137–139] interlayers,[140–142] and artificial SEI.[143–145] However, the sputtering of metallic lithium has almost not been studied. Indeed, only few works have been published. For example,[121,122] lithium layers of 10–40 µm thickness were deposited onto glass and SiO$_2$ substrates to investigate, by resonant nuclear reaction analysis, the Li diffusion into the substrates (**Figure 6**, left) and the lithium stability in air after being covered by a sputter-deposited thin-film of stainless-steel (Figure 6, right).[146,147]

Actually, lithium sputter targets and sputtering are very well known. However, to prove the viability of sputtering as a valuable tool for LMAs production, there is the need of a great fundamental improvement, particularly in the fabrication methods, configuration, and handling of Li sputter targets. In fact, conventional Li targets have several disadvantages due to the physical and chemical properties of metallic lithium itself (low

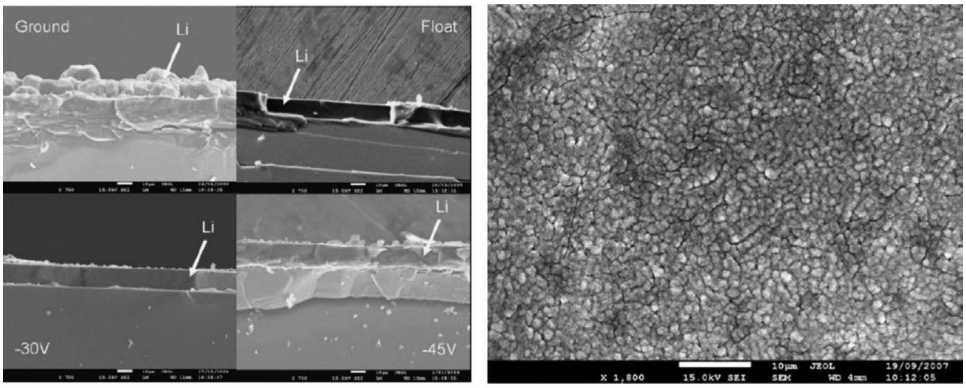

Figure 6. (Left) Cross-sectional SEM pictures of four samples (10 µm lithium) after 5 min of air exposure. Reproduced with permission.[146] Copyright 2008, Elsevier. (Right) SEM picture of the surface of a lithium sample covered by stainless steel (0.5 µm)/Li (10 µm)/SiO_2. Reproduced with permission.[147] Copyright 2009, Wiley.

melting point, low thermal conductivity, presence of passivating films on lithium surface). Moreover, a Li sputter target typically includes a Cu backing plate or similar support structure due to the malleable nature of Li; usually, the Li target heats up during the sputtering process and it can melt and/or have very poor adhesion onto the backing plate. Thus, improved methods are strongly needed of either fabricating lithium sputter targets, as suggested by Neumann et al.,[148] or improved associated methods of sputtering, as proposed by Mochalov et al.[149]

2.2.4. Thermal Evaporation

Thermal evaporation is a well-known and very basic technique for coating surfaces and substrates by both organic and inorganic thin layers.[150] The source material, which can be in a refractive wire form or placed into a metallic crucible, is electrically heated under UHV conditions. UHV is needed in order to avoid any possible chemical reaction of the source and to reach high purity of the deposited layers. The Joule heating, generated by the DC current, provides appreciable vapor pressures to the source material, which evaporates and condenses onto the substrate. A schematic of the thermal evaporation system is exhibited in Figure 4d.

This technique is especially suitable for materials with low melting points and high vapor pressure, as for instance lithium. Indeed, it is important to note that thermal evaporation is the preferred method to deposit lithium films,[151–157] due to lithium´s low melting point ($T = 180.5$ °C)[64] and high vapor pressure at low temperatures ($p = 10^{-4}$ Torr at $T = 407$ °C). As an example, cross-sectional Scanning Electron Microscope (SEM) images of $LiCoO_2$ /Li_3PO_4 /Li samples are shown in **Figure 7**, with thermally evaporated metallic Li anodes, as detailed by Matsuda et al.[152] However, in order to successfully evaporate lithium thermally, it is important that the material is not oxidized. In fact, LiO_x requires more initial power to break through the oxide layer and then melt the metal, and such high power may cause the remaining lithium metal to flash evaporate quickly. To avoid oxidation, lithium should be kept under an argon inert atmosphere. Moreover, it is important to identify at what electrical power the lithium melts. This can be done by manually ramping up the power and observing the material to determine when it melts. Once this power level is identified, it can be used as set point. Then, the power can be increased slowly until the desired deposition rate is reached. Furthermore, it is important to note that, once Li melts, liquid lithium may eventually alloy and damage the source itself, so the lifetime of these sources is unfortunately

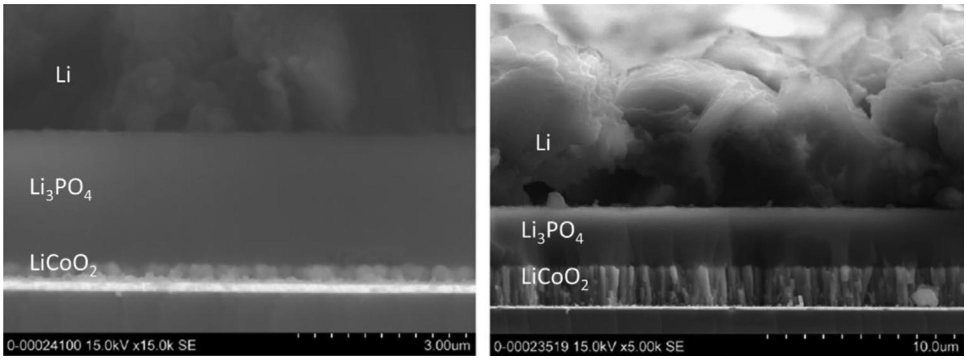

Figure 7. Cross-sectional SEM picture of samples made of $LiCoO_2$ (0.32 µm)/Li_3PO_4 (2.4 µm)/Li [left] and $LiCoO_2$ (2.2 µm)/Li_3PO_4 (3.4 µm)/Li [right]. Reproduced with permission.[152] Copyright 2018, Elsevier.

limited. Finally, since lithium has a relatively high vapor pressure one must carefully consider executing lithium evaporation in any deposition system. At already 300 °C, lithium has a significantly high enough vapor pressure to cause ppm level contamination in a vacuum system. For this reason, it is preferred to use only dedicated vacuum chambers for lithium deposition.

In summary, PVD techniques represent a more than interesting strategy to deposit thin layers of metallic lithium. **Table 1** provides the most commonly used parameters for the manufacture of metallic lithium. Among the different techniques analyzed, both EB-PVD and the sputtering process have yet to demonstrate their applicability beyond basic research, since due to limitations related to the nature of lithium itself, the extrapolation of these techniques far from the laboratory scale is quite complicated. Something similar occurs in the case of laser ablation. Although PLD is a highly versatile technique that allows to play with multiple parameters in order to prepare thin Li-metal layers with very different characteristics, it also presents an added complication related to the handling of lithium, which can be easily contaminated. Even so, it is possible to commercially obtain thin layers of metallic lithium prepared by PLD for implementation as anodes in lithium batteries.

Finally, thermal evaporation has been demonstrated to be the most appropriate PVD technique for obtaining thin films of metallic lithium, and it can hold a relevant position for the future of LMBs.[147–153] LMAs produced by PVD in general, including evaporation, are particularly good in terms of homogeneity and conformality of the surface, with defect-free surfaces being achievable. Moreover, PVD offers really good control of the thickness for lithium layers that could be in the range from nanometers to tens of micrometers, thus, being possible to overcome the current limitation on thickness for the conventional method. Additionally, intimate contact with the solid electrolyte would be ensured, which is often a problem in SSBs. Thermal evaporation is currently already used for the production of LMAs for thin film microbatteries. Besides, research and development and pilot line level equipment for lithium evaporation are commercially available. In fact, Canadian company Li Metal is intending to commercialize evaporated LMAs, having a pilot line already operational.

Table 1. Summary of metallic lithium deposition conditions using vapor-based techniques.

Technique	Conditions	Refs.
EB-PVD	Electron beam (magnetic field) High deposition rate Pressure: 10^{-7}–10^{-2} mbar Temperature: ≈2000 °C All types of material	[104]
PLD	KrF excimer laser (λ = 248 nm; 1.4 J cm^2 150 mJ^{-1}) Repetition rate: 2 Hz Deposition time: 1–4 h Pressure: ≈2×10^{-5} Pa Temperature: room temperature Target–substrate distance: 2–3 cm Substrate: 2 cm^2 stainless steel (SUS 316L)	[119]
Sputtering	Plasma (1–10 mA cm^{-2}; 10–200 kHz: 500–3 kV) High deposition rate Pressure: 10^{-7}–10^{-2} mbar Temperature: 100–500 °C Target–substrate distance: 6–16 cm Large area substrates	[122]
Thermal evaporation	DC current Pressure: 10^{-7} mbar Sample temperature: room temperature Target–substrate distance: ≈5 cm	[150]

2.3. Liquid-Based Fabrication Technique

Liquid-based technique is another promising method to prepare LMAs for LMBs. By taking the advantage of lithium relatively low melting point,[64] it can be transformed into a liquid state easily in an anaerobic atmosphere. It can be then deposited on a substrate/surface by using standard methods, such as dip coating, spray coating, or doctor blading. However, one disadvantage that must be considered when dealing with melted lithium is its low wettability on various relevant substrates due to its high surface energy, being the major technological challenge of this approach. Regulating the wettability between liquid – Li and the scaffold materials is crucial in this process. Several researchers have already noticed the importance of controlling the lithiophilicity[158,159] and have classified the different approaches as chemical strategies;[160] coatings on the host materials, doping with lithophilic species or alloying the Li metal with polar functional groups, and physical strategies, i.e., modifying the surface roughness[161] and adjusting the surface energy.[162]

It has been demonstrated in the last years that a combination of lithiophilization and inexpensive liquid coating techniques could be suitable for the battery manufacturing industry. In 2016, the research group led by Cui[163] described a straightforward melt-infusion approach to effectively encapsulate Li inside a porous host scaffold based on 3D carbon. They overcame the low wettability of liquid-lithium by using a lithiophilic Si-coating. Indeed, the porous host carbon scaffold was directly coated by Si. The melted-Li was then encapsulated into the 3D-matrix Si/C structure. By doing so, a Li-composite-like material was created, which showed high gravimetric (≈2000 mAh g^{-1}) or volumetric (≈1900 mAh cm^{-3}) capacities. The reported strategy led to very good battery performance with low interfacial impedance, stable voltage profile, and long cycle life. Despite a minimal volume change was observed, due to the host scaffold that encapsulated the lithium-metal, this did not impact the high conductive surface area and the good electrolyte/electrode interface stability. Compared with a host-less LMAs, this Li/C composite electrode showed multiple advantages and therefore opened a new path for overcoming the intrinsic problems of LMBs.

In 2018, Reinhart et al.[86] reported a large number of lithium-anode processing techniques including melt processing combined with polymer-based foils.[164] lithium was deposited into nonporous electrolyte or infiltrated by melt infusion from the uppermost surface of the porous electrolyte structure. A lithiophilic coating and/or surface treatment was also in this case needed to increase the wettability of the electrolyte against Li. Moreover, the atmosphere where all these processes took part had to be finely controlled due to the high reactivity of liquefied lithium.

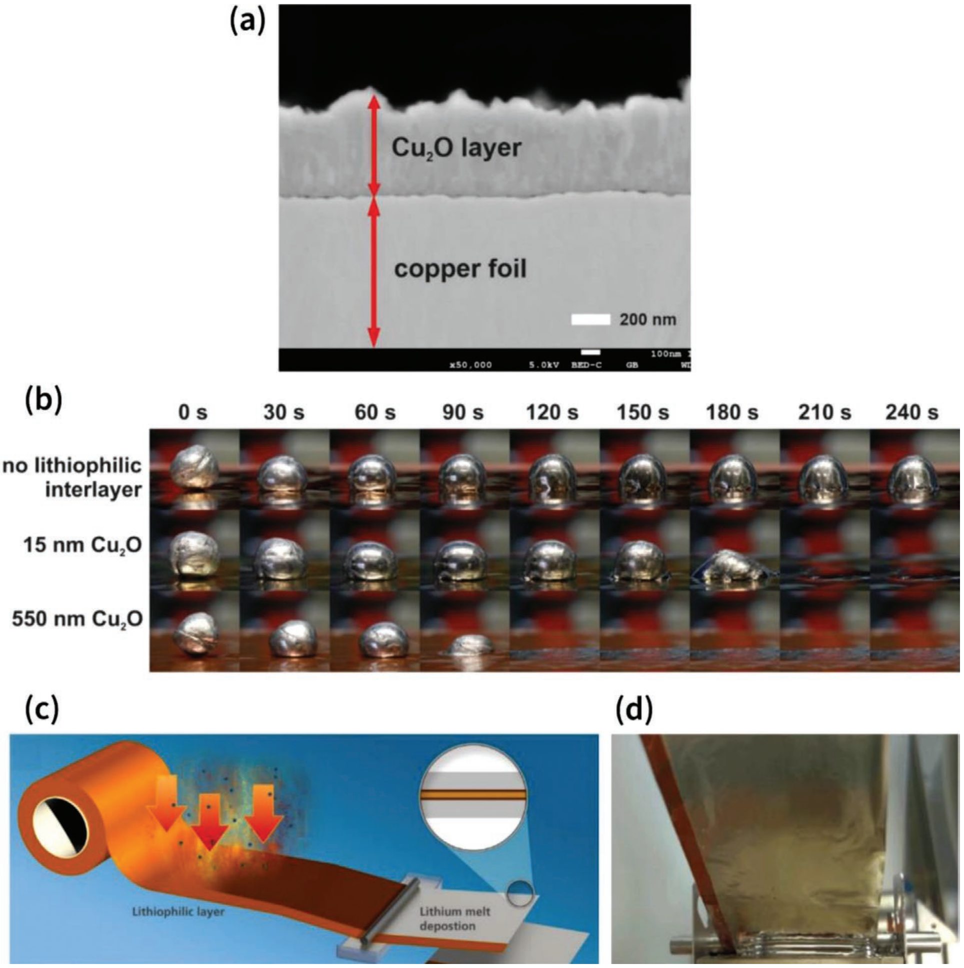

Figure 8. a) Scanning electron microscope cross section image of a Cu_2O layer (450 nm) on copper foil (6 µm). b) Photographs of molten lithium on copper foil with and without Cu_2O layer. c) Schematic of the lithium-melt deposition process. d) photograph of the coating tool. Reproduced with permission.[168] Copyright 2022, Elsevier.

In 2022, melt-induced stacking[165,166] followed by vacuum deposition and melt-induced infusion[167] were considered by Hatzell et al.[166] as promising techniques for manufacturing LMAs. Melt-induced infusion allows plastic flow of lithium resulting in better contacts with the electrolyte. Even though tough thin lithium layers are achieved, it is a very expensive method for large-scale production.

Recently, Kaskel et al.[168] have proposed an alternative strategy based on lithium melting processing to obtain thinner and longer lithium foils. They have reported the absence of publications referring to production technologies or scalable concepts for thin anodes, whereas a vast amount of those could be found on cycling at small scale.[6,169–173] Metallic lithium has low mechanical strength, thus, as mentioned earlier, methods such as extrusion and rolling have some limitations when thin (e.g., < 50 µm), wide (e.g., > 100 mm) and long (e.g., > 10 m) foils or even coils are required.[174] Moreover, handling lithium thicknesses below 50 µm remained challenging. As mentioned above, metallic lithium is highly reactive and sticks on tools or rolling cylinder surfaces.[78] Some solutions, as using lubricants have been proposed, but lead to side-reactions and to nonperfectly controlled surface coatings.

In this respect, Kaskel et al.[168] have introduced a disruptive deposition process for thin lithium metal coating on thin copper current collector (CC) foils. The low wettability of the liquid lithium has been tackled by using a thin lithiophilic interlayer based on the mild thermal oxidation of the copper CC. The resulting Cu_2O layer (**Figure 8**a) dramatically enhances the wettability of the copper substrate, by taking advantage of the reactive conversion of Cu_2O by elemental lithium. The oxidation reduction reaction that occurs is listed below:

$$Cu_2O + 2Li \rightarrow 2Cu + Li_2O \tag{4}$$

Upon the interaction of molten lithium with the Cu_2O layer, the Cu_2O is consumed leading to Li_2O and Cu species which are no longer present as a compact film and embedded lithium-metal in the interface region Cu-substrate/lithium coating. The liquid-lithium coatings were carried out in an inert argon atmosphere by roll-to-roll dip coating-inspired processes. With this new process the lithium-thickness could be tuned in a wide range (1–30 µm). The coating width was manipulated to provide uncoated edges for CC tabs. In addition, the resulting lithium surface offered high purity, allowing specific functionalization.

The effect of the Cu_2O lithiophilic layer can be observed in Figure 8b where solid spherical lithium samples were placed on hot substrates with and without lithiophilic interlayer with different thicknesses. For the pure copper foil, no lithium spreading was observed after the melting, whereas for the two explored Cu_2O thicknesses a perfect wetting was found after a time inversely proportional to the thickness.

Figure 8c,d shows this coating process schematically where the substrate is in contact with the liquid-lithium at a defined angle. The evaluation in prototype solid batteries showed high electrochemical lithium utilization and no detrimental effects. Therefore, Kaskel et al.[168] proved the feasibility of the fabrication lithium foil by melting technique using a lithiophilic coating on the substrate.

From a completely different approach, Livent company developed a printed lithium foil to be used as LMA, which is inspired by the current Li-ion slurry-based technology for electrode production.[175,176] The formulation of the slurry is composed of lithium metal powder, rheology modifiers, and a solvent, which is then spread on a current collector (or, potentially, on the separator or on a solid-state electrolyte) by means of slot die coater, to be finally calendered. The thickness of the produced lithium foil ranges from 10 to 50 µm. Beyond the possibility of producing thinner LMAs than with the conventional method, printable technology also gives higher flexibility on widths. The fact that the process is basically identical to current electrode production technology is the main benefit of this original method.

To summarize this section, melt processing of lithium is an alternative enabling technology not only for achieving high energy density on system level but also because opens important opportunities for subsequent native surface engineering adapted to various solid state and liquid electrolyte interfaces in future. Costs of production increase exponentially when a high-quality layer and thickness-controlled layer can be made on top of Cu current collector. A reduction of the anode thickness by using ultrathin lithium metal films is a key requisite to achieve a significant overall reduction of thickness and, thus, higher energy densities on cell level.

2.4. Electrodeposition

Beyond the previous method described for LMA production, metallic lithium films can also be produced by means of electrochemical processes. The origin of the electrodeposition of metals dates back to the 19th century, to the days when Volta invented the first electrical battery, and it has been developed and implemented in different industries since then. Electrodeposited metal films are obtained by applying a certain current between two electrodes, which are connected to an external electrical power supply and immersed into an electrolyte. Metal film grows on top of the negative electrode via a reduction process, whereas the positively polarized electrode is oxidized. At lab-scale development, this electrochemical process is performed in relatively small cells or containers, using either two or three electrode configurations (to control the potential of each electrode). On a commercial scale, however, big tanks in the order of meters are used, where even continuous plating in reel-to-reel format can be implemented.[177]

In contrast to other metals, metallic lithium films produced by electrodeposition are still not commercially available, though this method would bring several benefits if implemented for LMA production. First of all, high temperatures and toxic gases produced with the current conventional method would be avoided. Moreover, the production cost could potentially be lower due to lower process temperatures and lower raw material costs, among others. Additionally, this technique would allow the production of lithium films with a thickness much below the limit of current extrusion method and higher flexibility in widths. On the negative side, compared to other metals produced by electrodeposition, the process would need to be done in dry-room atmosphere and probably using hazardous electrolytes, due to the properties of lithium.

Although Li foil usually used as LMA is mainly manufactured by extrusion from ingots, the electrodeposition of lithium on metallic current collectors has also been considered and studied to produce thin lithium films that could be used as electrodes in LMBs. In the 1990s, Kanamura et al.[178] studied the electrodeposition of lithium on nickel substrate in non-aqueous electrolytes. They observed that hydrofluoric acid (HF) traces on the electrolyte were beneficial to obtain more homogeneous deposition of the lithium on the substrate. Adding a controlled amount of HF in $LiClO_4$ salt-based organic electrolyte, they obtained a smoother surface formed of regular spherical deposits, being the outermost surface mainly composed of LiF.[178] Same group further investigated the impact of the formation of such outermost layer on the morphology of electrodeposited lithium, concluding that the beneficial role is limited to the first deposition, evolving toward dendritic Li deposition over time.[179] Hence, the LiF containing layer would enable the deposition of homogeneous Li films that could be used as LMAs, though it would not overcome limitations related to Li metal electrode degradation upon cycling in conventional electrolytes.

More recently, other researchers have also studied the effect of controlled amounts of impurities on the deposition morphology and homogeneity of electrodeposited lithium films. The positive effects of controlled amounts of H_2O added to $LiPF_6$ salt based organic electrolyte were demonstrated by different groups.[180,181] Both the amount of added H_2O and the time elapsed between the addition and the electrodeposition were demonstrated to be crucial to obtain a better homogeneity and deposition morphology. The beneficial effect of H_2O traces for lithium electrodeposition has also been shown with tetraglyme-based electrolytes, where improved Coulombic efficiencies (CE) were obtained for controlled amounts of H_2O traces added to the electrolyte.[182]

Many recent studies have demonstrated the great importance of electrolyte composition on deposition morphology and stability of LMA upon cycling. Despite being focused on the use of LMA in actual cells and not in the production of lithium films, the results obtained in these studies are also relevant for the production of LMAs by electrodeposition and could be useful to identify improved electrolyte formulations to optimize the production process. For instance, more compact circular island-like deposition is observed when using ether-based electrolytes, whereas higher surface area whisker-like or mossy lithium is observed with carbonate-based electrolytes.[48] Conducting salt and its concentration does also highly influence the deposition morphology of lithium. High concentration electrolytes (HCE), and, the practically more viable localized high concentration electrolytes (LHCE), form much smoother and less porous surfaces compared to conventional electrolytes.[45,54,183] Moreover, additives can also be used to modify lithium plating behavior. Besides H_2O and HF mentioned before, other additives have also been explored to form a LiF layer that would form a more homogeneous and stable lithium deposition, among which fluoroethylene carbonate (FEC) stands out.[54] Other additives, such as $LiNO_3$[184] or $CsPF_6$,[185] have also been demonstrated to have a profound impact on lithium deposition morphologies in LMBs.

The effect that other parameters have on the electrodeposited films, such as the distance between electrodes or current densities used, has also been explored. The relation between applied current density and morphology of the deposited layer has been described in many works. Columnar growth of lithium (**Figure 9**a–f) was observed in many studies for the best electrodeposition conditions,[180,181,186,187] which was always linked to the formation of LiF layer on the surface of the copper substrate, in line with the results obtained in the 1990s.

Moreover, the correlation between nuclei diameter and applied current density has also been confirmed,[180,187] with an inversed relationship between deposits diameter and applied current density, in good agreement with the nucleation theory.[188] The effect of the distance between the electrodes during the electrodeposition process was recently studied by Chae et al.[189] They observed an evolution of deposited lithium morphology with the distance between the electrodes, with inhomogeneous morphology for short distances and homogeneous deposition with regular spherical deposits beyond certain separation. They suggested that this phenomenon is nested on high Li-ion concentration region generated near the counter electrode during the electrodeposition process.[189]

The electrodeposition processes described in the works cited so far, rely on a metallic lithium counter electrode as lithium source to deposit a thin lithium layer on the working electrode in a controlled manner. Such dependency on a metallic lithium counter electrode would imply the need to produce metallic lithium previously by other means. Being able to produce electrodeposited metallic lithium film using a lithium source other than metallic lithium counter electrode would be highly beneficial if this technology is going to be considered for the production of LMAs from a commercial standpoint. From this approach, Mashtalir et al.[186] described a process based on a circulating aqueous solution containing Li_2CO_3 as feedstock (Figure 9g), which is separated by a ceramic membrane from the $LiPF_6$ based electrolyte and Cu working electrode.[186] Using this original setup, they demonstrated the deposition of high-purity lithium metal films with different nucleation morphologies depending on the current density that was applied.

Besides academic studies on different methods and the impact of different parameters for obtaining electrodeposited metallic lithium films, interest has also been directed toward the commercialization of electrodeposited LMAs. Alpha-En, a US-based company, is in the process to scale-up and commercialize electrodeposited lithium electrodes based on

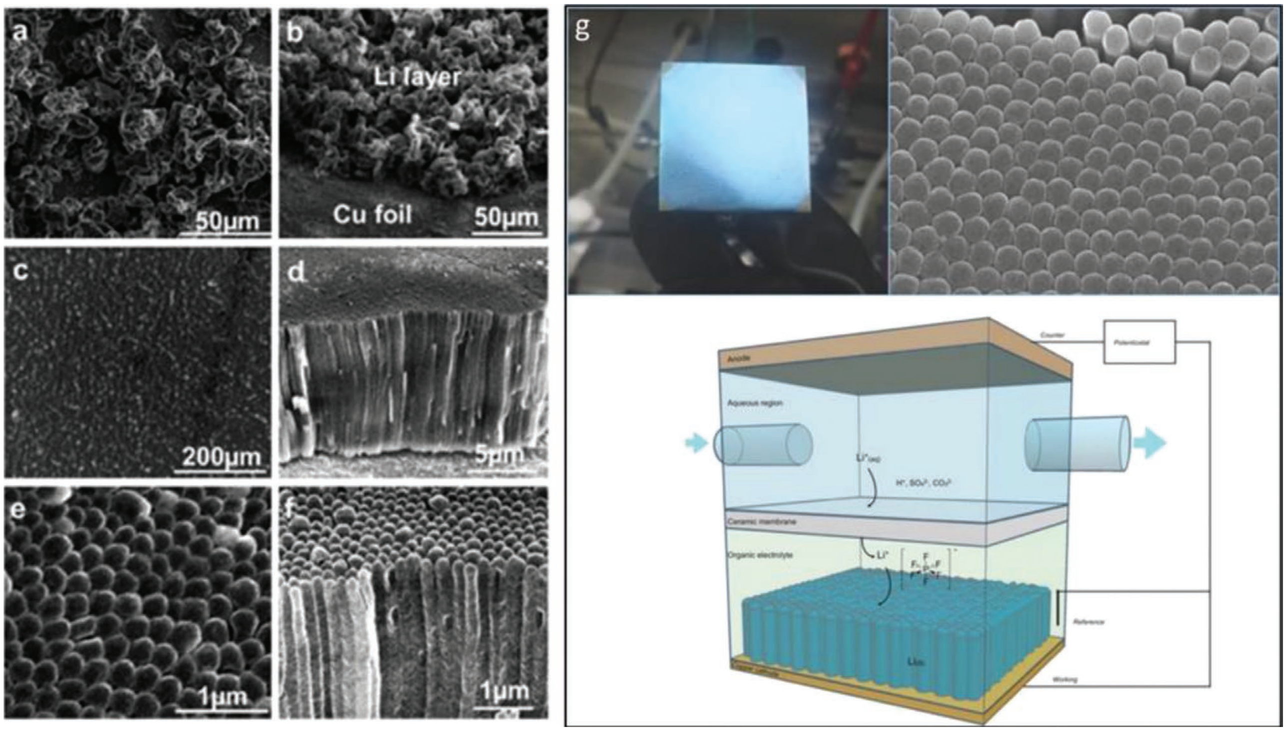

Figure 9. Electrodeposition of metallic lithium on Cu CCs. a–f) SEM images of lithium deposited with a–c) and without d–f) H_2O additive. Reproduced with permission.[180] Copyright 2015, Elsevier. g) Visual and SEM images of electrodeposited lithium and configuration used by Masthalir et al. Reproduced with permission.[186] Copyright 2018, American Chemical Society.

their patented technology,[190–192] which is based on a method described above.[186] Pure Lithium, another US based company, is also developing their patent-pending technology for the electrodeposition of lithium electrodes and intending to implement it in their own cell development. Their electrodeposition process is based on using Li salts, such as Li_2SO_4 or Li_2CO_3, as lithium source to deposit it in copper current collectors through a polymer membrane. Beyond these emerging entities, well stablished companies on the lithium and battery markets[193,194] have also demonstrated interest on the electrodeposition process for LMA production.

2.4.1. Anode-Less Concept

The cathodes currently used in Li-ion cells and most of the next generation cathodes under development already contain the lithium source in their composition when the cell is assembled. In most of the LMBs, LMA is included as an additional lithium reservoir (excess), which is required due to the high irreversibility of the electrochemical process upon cycling that produces a constant loss of lithium inventory. Ideally, if such inefficiencies are overcome and close to 100% CE is achieved, there would be no need to have an additional lithium source, and, thus, the cell could be assembled without LMA, having only the CC on the negative electrode side. In such configuration, which is named anode-less or anode-free, LMA would be formed during the first charge (and subsequent charges). Hence, this could be described as an in situ electrodeposited LMA.

The anode-less concept has many benefits, among which the most obvious is the increase on specific energy and energy density. Additionally, having less amount of lithium within the cell would be beneficial from the safety point of view, and it could also make the production process simpler (avoiding lithium processing) and less expensive.

The anode-less concept for LMBs was demonstrated two decades ago by Bates et al.,[153] who developed a LMA free thin-film battery prepared by PVD techniques in which lithium from $LiCoO_2$ cathode was deposited in the copper negative CC during charge. This kind of thin film microbattery, however, contains low areal capacity. When the anode-less concept is implemented in bigger cell formats in the order of mAh cm^{-2} cathode active material loading, the inefficiencies during the lithium plating/stripping on copper CC leads to a rapid degradation of the cell. Hence, many works have focused lately on the design of anode-less cells that would improve such limitations from different approaches, including solid and liquid electrolyte development, study of artificial SEI layers and engineering of CC and host materials. Here, only the most relevant examples at CC and 3D host level will be described since the rest are beyond the scope of this review work.

Cu Current Collector Modification: Copper CC (Cu CC) is commonly used in the negative electrode in Li-ion battery cells, and for this reason, it is the most usual choice in anode-less studies. However, due to the inefficiencies of lithium stripping-plating process on it, the use of bare copper foil CC is not a viable option. Therefore, many works have been oriented toward the development of modified Cu CCs with modified surface. Some of them have focused on the improvement of copper surface by modifying its main surface crystal orientation,[195–198] by pre-depositing some lithium,[199,200] or by depositing a thin layer of another material,[201,202] aiming to improve the nucleation and deposition morphology of lithium on the CC and lifetime of the cell. Some alloys formed by lithium with other metals have been demonstrated to be more lithiophilic and, thus, favor the lithium deposition in comparison to copper. Some of the examples include Zn,[203–205] Al,[206,207] B,[208] Sn,[209,210] or Ag,[211,212] which showed, in general, a lower nucleation overpotential and more homogeneous lithium deposition.

Beyond Cu CC, other modified metallic CCs have also been used for anode-less cell development. One of the works that attracted most interest, published by Lee et al.,[213] was based on the use of SS as negative current collector in an all-solid-state cell in which a thin composite layer was added at the SS CC and the SEI. The composite, formed of carbon black with silver nanoparticles, was key for enabling a stable lithium deposition with CE above 99.8% for high loading cathodes (>6.8 mAh cm^{-2}) demonstrated at 0.6 Ah prototype pouch cell level.

Current Collector and Hosts: Another area of study for lithium metal anode-less batteries is the development of 3D structured CC or hosts. A 3D structure could potentially increase the surface area for deposition of lithium, which would reduce the current densities on the CC. Furthermore, certain structures could deal better with the large volume expansion of the LMA during cycling. One of the most common strategies among 3D CC development is the design of 3D Cu CCs. In 2015, Yang et al.[214] showed a 3D CC with a submicrometer-sized skeleton and porous structure capable of improving lithium plating behavior (**Figure 10**j). The submicrometer skeleton was produced starting from planar Cu foil, which was chemically treated by submerging in a solution to obtain a self-assembled CuO structure, then dehydrated and reduced to have the final porous copper CC. Using this porous CC, lithium was observed to grow within the submicrometer-sized Cu skeleton, filling the pores of the 3D CC and avoiding dendritic growth. From a process also based in chemical solution, Lu et al.[215] prepared a Cu CC made of interconnected nanowires that enabled the controlled lithium growth. Another method to fabricate porous Cu CC is the electrochemical dealloying of Cu-Zn tape, with which more stable SEI formation, improved CE and lifespan and enhanced mechanical properties have been reported.[216,217]

CCs with ordered structures have also been reported as suitable hosts for efficient lithium deposition. An electrophoretic deposition of a colloidal template followed by Cu electrodeposition was reported by Tang et al.,[218] resulting in a 3D ordered macroporous Cu structure after the template was removed. A similar approach using a dynamic H_2-bubble template via electrodeposition to obtain porous CC formed of Cu dendritic superstructures was also described.[219] Besides, a more conventional slurry-based method, similar to the one commonly used for electrode production, was described by Chen et al., with which micrometric Cu particle structure was casted on Cu foil.[220] Development of vertically aligned microchannels[221] or Cu pillars[222] (Figure 10e–i) have also been demonstrated as 3D CCs, produced by laser microprocessing, and templated electrodeposition process, respectively. The use of Cu meshes has also been an approach used by different groups, with different processing including pressing lithium into the Cu mesh

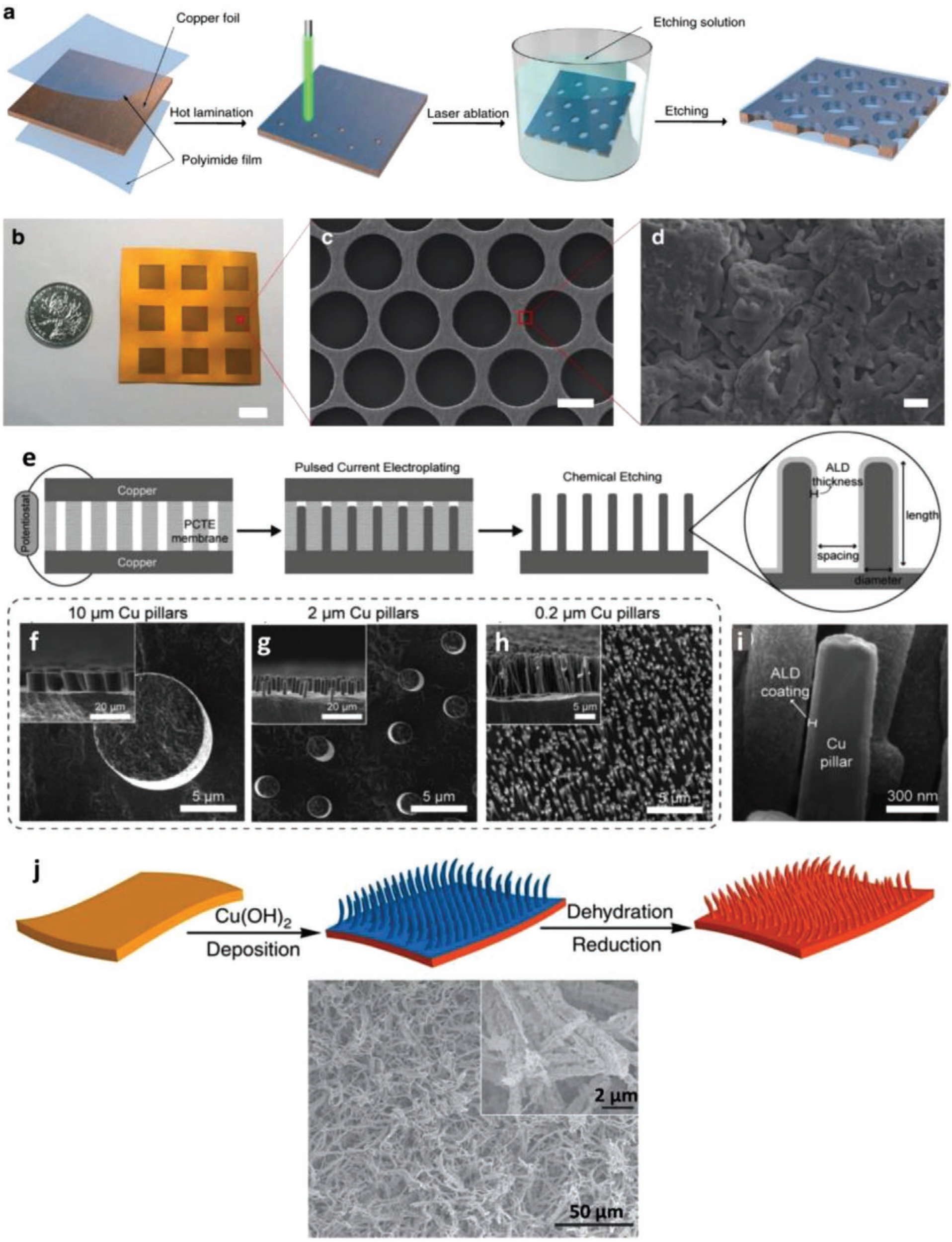

Figure 10. a–d) Circular holes on Cu foil by laser patterning: a) schematic representation of the process. b–d) Visual and SEM details of the patterned foil. Reproduced with permission.[223] Copyright 2018, Springer Nature. Scale bars in (b–d) are 1 cm, 100 µm, and 1 µm, respectively. e–i) Vertically aligned Cu pillars: e) schematic representation of the processing method; f–h) SEM images of pillars with different diameter; i) detail of the ALD coating on Cu pillars. Reproduced with permission.[224] Copyright 2020, Elsevier. j) Schematic representation of the method to produce 3D Cu CC with submicrometer-sized skeleton and SEM image of the 3D CC. Reproduced with permission.[214] Copyright 2015, Springer Nature.

to form a composite, changing facet orientation for improved lithiophilicity,[195] patterning Cu foil with circular holes by laser patterning (Figure 10a–d),[223] or implementing different coatings in a commercial 3D mesh to induce homogeneous lithium deposition across the CC.

Beyond Cu CCs, 3D collectors and hosts made of other materials, either conductive or nonconductive, have also been engineered. Alternative metallic CCs have been explored by modifying their structure and surface by different methods. These include, for instance, the use of carbon-nitrogen modification of a SS mesh as a 3D host (**Figure 11**a–g),[224] or the development of patterned Ti foil with ZnO nanowire arrays deposited by hydrothermal reaction method. Another strategy to produce a conductive host consists of directly casting a porous layer on top of the CC, such the work reported by Liu et al.[225] where a layer of $LiNO_3$, carbon black and Polyvinylidene fluoride (PVDF) was demonstrated as host.

Nonconductive layers can also be effective in homogenizing the Li-ion concentration across the 3D CC. Based on that concept, Liu et al.[226] developed an engineered polyamide coated

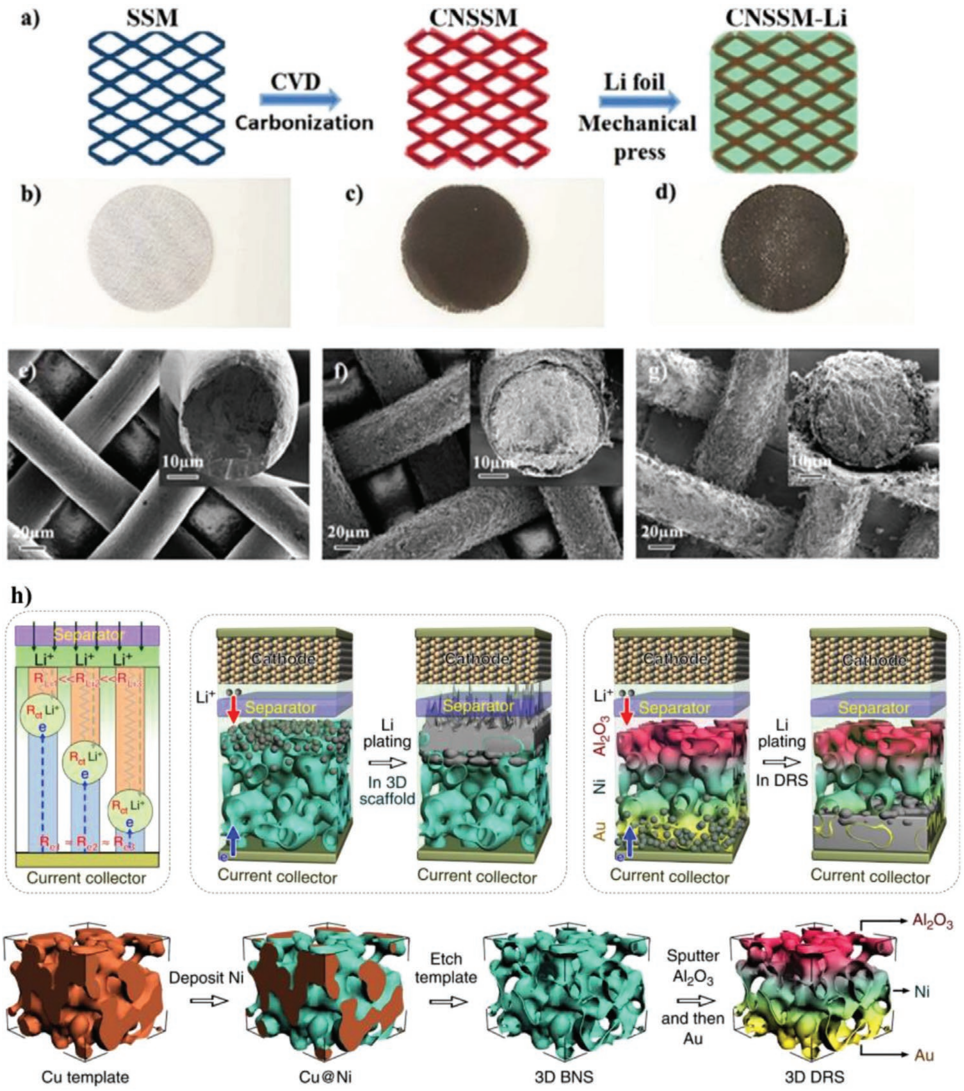

Figure 11. a–g) Schematic representation of processing, visual top images, and SEM images of carbon-nitrogen modification of a stainless steel mesh (SSM), conductive carbon-nitrogen modified stainless steel mesh (CNSSM) carbon-nitrogen modified stainless steel mesh and lithium composite electrode (CNSSM-Li). Reproduced with permission.[224] Copyright 2020, Elsevier. h) Schematic representation of Ni scaffold with lithiophilic gradients and its benefits upon cycling. Reproduced with permission.[230] Copyright 2019, Springer.

SS-CC made of small channels to stabilize lithium plating by lithium deposition within the channels more homogeneously. Other works that have focused on nonconductive hosts with similar strategy include the use of 3D porous polymelamine and lithium composite,[227] or the use of a Cu CC covered by a cloth such as polyethylene terephthalate-based fabric[228] or modified glass fiber with large functional groups.[172] Despite being designed for a different application, dual LiF/Li_2O layer was reported as a shell for stabilizing lithium spheres which were then electroplated on graphite as a prelithiation strategy to compensate the active lithium loss due to the formation of SEI.[229]

More complex designs include the use of several coatings that induce conductivity and lithiophilic gradients across the 3D current collector. Pu et al. developed a Ni scaffold with top and bottom layers consisting of Al_2O_3 and Au, respectively, which were deposited by sputtering Cu CC (Figure 11h).[230] A similar concept, using same coating materials, was also reported on 3D Cu mesh.[231]

Besides structured and modified 3D metallic CCs, carbon-based hosts have also been proposed to efficiently plate metallic lithium. Although some works use only the carbon-based material as a host, such as graphene particles,[232] most of reported methods include the use of additional materials or layers to improve lithiophilicity, guide lithium deposition or even limit the reactivity with the electrolyte. Xie et al.,[233] for instance, coated the surface of hollow carbon spheres with Al_2O_3 using atomic layer deposition (ALD). Several other groups have reported the addition of metallic nanoparticles or nanowires into the carbon-based host to facilitate lithium nucleation and lower the overpotential.[234–236] Additionally, processing of hybrid carbon-based electrodes that enable both intercalation and controlled electrodeposition of lithium have also been explored by engineering 3D electrodes based on graphitized carbon fibers or spherical granules.[237,238]

3. Conclusions and Perspectives

In conclusion, current production of lithium foil used for LMAs relies on a process that did not change considerably for around a century and presents some limitations in relation to its sustainability and the quality of the lithium foil that is produced. As a matter of fact, the quality of the lithium foil produced by the conventional method (i.e., electrospinning, extrusion, and rolling) is good enough for its use in primary lithium cells, which has been the main use in batteries up to date. However, it does not meet the requirements to be used as a LMA in secondary LMBs, as for instance, the high current density demanded by the automotive industry. First, the quality of the outermost surface of the lithium presents some deficiencies that jeopardize its efficient performance during continuous plating and stripping processes. Due to the reactivity of lithium, the outermost surface of the lithium shows a relatively thick layer of material, which composition is other than metallic lithium, generally formed of an inner thin oxide layer followed by a thicker lithium carbonate layer. In addition, for lithium foils with thicknesses below the extrusion limit (generally around 100 µm), a lubricant is used during the rolling process, which produces contamination in the surface in the form of Si-based traces. The morphology and structure at the surface of the lithium foil can also influence its efficient performance during cycling. The presence of relatively big grains on the surface with different orientations, and the roughness produced by the grain boundaries and defects from the extrusion and rolling processes can also be detrimental. Furthermore, the dimensions of the foil obtained by the conventional method are an additional limitation. The need for thinner LMAs with only few micrometers in thickness is beyond the limits of the technique. The maximum limits on the width from the extrusion step are also a limitation when big dimension cells are designed, particularly those oriented toward the use in Electric Vehicles.

Hence, the need for alternative methods to produce lithium films to be used as LMAs is striking. Different approaches can be used to find an alternative method, which were classified in this work as vapor based, liquid based, and electrodeposition. Suitability as a production method at large scale would not depend only on the properties of the product, the feasibility of the method at industrial scale would also need to be considered. The trade-off between properties and process feasibility is visually represented in **Figure 12**.

Among the vapor-based techniques, thermal evaporation is the best choice to be implemented at large scale. In fact, this method is already used for LMA production in thin-film microbatteries that are commercial, and prototype level equipment for the production of evaporated lithium reels to be used as LMAs in larger cells is also a reality nowadays. One of the main strengths of this method relies on the quality of the lithium that is produced, both from the compositional and morphological points of view. It would be a particularly suitable option if the lithium deposition process is combined with the deposition of a protective layer in the same vacuum process, that would help to stabilize the anode-electrolyte interface and boost the performance of LMBs. The other main benefit would be the possibility to reduce the thickness of the LMA, into a range that

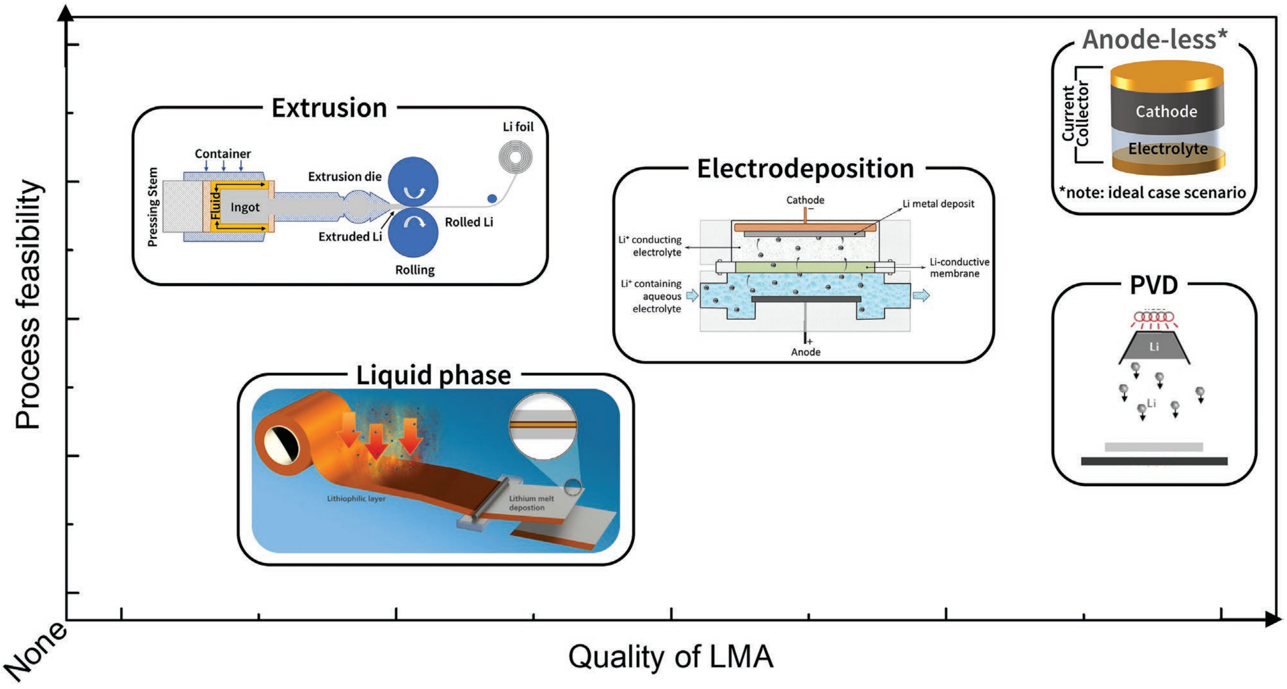

Figure 12. Trade-off between properties and process feasibility for the different alternative LMA production methods. Liquid phase figure, reproduced with permission.[168] Copyright 2022, Elsevier. Electrodeposition figure, reproduced with permission.[186] Copyright 2018, American Chemical Society.

could go from nanometer scale up to tens of micrometers, with a good control of the thickness. The need of high vacuum systems, which require high investment and maintenance costs, could be considered as a drawback compared to other alternatives and could limit the implementation of this techniques at large scale.

Liquid-based methods described in this work, despite being a simple approach that does not require complex systems to be implemented, lack the accurate control of the thickness and surface morphology that other techniques offer. Moreover, if implemented at large scale, having large amounts of lithium in molten state would raise safety concerns. Nevertheless, a very specific case is the slurry-based method developed by Livent (different to molten lithium process), which could easily be scaled up since the process is very similar to that used nowadays for Li-ion electrode manufacturing. The limitation of this method might be in the quality of the lithium, which would be similar to that of the extruded lithium foil.

Electrodeposition offers a good trade-off between the quality of the lithium layers that are produced and the viability of the process. It is a mature technology that has been used industrially for many years to produce metallic layers. For lithium, at experimental level, pure layers with very homogeneous surfaces and really good control of surface morphology and thickness have been demonstrated. Thus, this technique would potentially be one of the best alternative choices for the conventional method to produce LMAs. If the developments that use lithium salts, such as Li_2CO_3, as source of lithium during the electrodeposition process can be demonstrated at large scale, this method would be particularly attractive from an industrial point of view.

Anode-less concept, which could be described as an in situ electrodeposition of the LMA, would be the ideal case scenario for the LMBs that have the lithium source in the cathode active material when the cell is assembled.

For this configuration to be competitive, though, very high efficiencies are needed, for which lithium plating and stripping mechanism needs to be homogeneous, ordered and degradation-free during long cycling. To achieve that, the development of advanced current collectors with defect-free and lithiophilic surfaces is of paramount importance. Some promising performances have been reported, as described in the corresponding section, although the scalability of the process would need to be studied to see if they are real alternatives that could be widely implemented. Furthermore, 3D current collectors and host materials are also being explored for anode-less LMBs, being their main advantages the higher surface area and space of the 3D structures that can help with lower current densities and dealing with the large volume changes, respectively. Many different processing techniques and materials have been reported to show promising results. It is important, though, to ensure that the benefit of using LMA in terms of energy density and specific energy is not lost with the additional space and weight of 3D current collectors.

In summary, although other developments such as the engineering of interfaces or development of advanced electrolytes and cathodes are also crucial to enable the LMBs, LMAs with improved quality produced by feasible methods are a requirement. Many alternatives are on the table and progress is being made both at research and scale-up and commercialization levels, which suggests that this is going to be a crucial topic for the development of future generations of lithium-based batteries.

Acknowledgements

All the authors are thankful to Miguel Ángel Muñoz Márquez for the fruitful scientific discussions and to Miriam Gutiérrez Granado for her substantial design contribution. I.R.L. acknowledges the support of the Ministerio de Ciencia, Innovación y Universidades (No. PID2019-107468RB-C21) and Gobierno Vasco/Eusko Jaurlaritza (No. IT1546-22). This project has received funding from the Basque Government within the ELKARTEK 2021 call (project CICe2021) under the application number KK-2021/00064.

Conflict of Interest

The authors declare no conflict of interest.

Keywords

anode-less, electrodeposition, lithium metal anodes, lithium metal batteries, lithium processing

Received: November 4, 2022
Revised: December 16, 2022

[1] J. B. Goodenough, K. S. Park, *J. Am. Chem. Soc.* **2013**, *135*, 1167.
[2] M. Li, J. Lu, Z. Chen, K. Amine, *Adv. Mater.* **2018**, *30*, 1800561.
[3] T. M. Armand, J.-M. Tarascon, *Nature* **2008**, *451*, 652.
[4] N. Nitta, F. Wu, J. T. Lee, G. Yushin, *Mater. Today* **2015**, *18*, 252.
[5] A. Mauger, C. M. Julien, J. B. Goodenough, K. Zaghib, *J. Electrochem. Soc.* **2020**, *167*, 070507.
[6] X. B. Cheng, R. Zhang, C. Z. Zhao, Q. Zhang, *Chem. Rev.* **2017**, *117*, 10403.
[7] G. Zou, H. Hou, C. W. Foster, C. E. Banks, T. Guo, Y. Jiang, Y. Zhang, X. Ji, G. Zou, H. Hou, T. Guo, Y. Jiang, X. Ji, C. W. Foster, C. E. Banks, Y. Zhang, *Adv. Sci.* **2018**, *5*, 1800241.
[8] J. Chen, G. Zou, W. Deng, Z. Huang, X. Gao, C. Liu, S. Yin, H. Liu, X. Deng, Y. Tian, J. Li, C. Wang, D. Wang, H. Wu, L. Yang, H. Hou, X. Ji, *Adv. Funct. Mater.* **2020**, *30*, 2004302.
[9] D. H. Seo, J. Lee, A. Urban, R. Malik, S. Kang, G. Ceder, *Nat. Chem.* **2016**, *8*, 692.
[10] K. Luo, M. R. Roberts, R. Hao, N. Guerrini, D. M. Pickup, Y. S. Liu, K. Edström, J. Guo, A. V. Chadwick, L. C. Duda, P. G. Bruce, *Nat. Chem.* **2016**, *8*, 684.
[11] B. Qiu, M. Zhang, L. Wu, J. Wang, Y. Xia, D. Qian, H. Liu, S. Hy, Y. Chen, K. An, Y. Zhu, Z. Liu, Y. S. Meng, *Nat. Commun.* **2016**, *7*, 12108.
[12] H. Yu, H. Zhou, *J. Phys. Chem. Lett.* **2013**, *4*, 1268.
[13] B. Li, D. Xia, *Adv. Mater.* **2017**, *29*, 1701054.
[14] A. Manthiram, J. C. Knight, S. T. Myung, S. M. Oh, Y. K. Sun, *Adv. Energy Mater.* **2016**, *6*, 1501010.
[15] M. Freire, N. V. Kosova, C. Jordy, D. Chateigner, O. I. Lebedev, A. Maignan, V. Pralong, *Nat. Mater.* **2015**, *15*, 173.
[16] W. Liu, P. Oh, X. Liu, M. J. Lee, W. Cho, S. Chae, Y. Kim, J. Cho, *Angew. Chem., Int. Ed.* **2015**, *54*, 4440.
[17] A. M. Colclasure, A. R. Dunlop, S. E. Trask, B. J. Polzin, A. N. Jansen, K. Smith, *J. Electrochem. Soc.* **2019**, *166*, A1412.

[18] K. H. Chen, M. J. Namkoong, V. Goel, C. Yang, S. Kazemiabnavi, S. M. Mortuza, E. Kazyak, J. Mazumder, K. Thornton, J. Sakamoto, N. P. Dasgupta, *J. Power Sources* **2020**, *471*, 228475.
[19] S. Ahmed, I. Bloom, A. N. Jansen, T. Tanim, E. J. Dufek, A. Pesaran, A. Burnham, R. B. Carlson, F. Dias, K. Hardy, M. Keyser, C. Kreuzer, A. Markel, A. Meintz, C. Michelbacher, M. Mohanpurkar, P. A. Nelson, D. C. Robertson, D. Scoffield, M. Shirk, T. Stephens, R. Vijayagopal, J. Zhang, *J. Power Sources* **2017**, *367*, 250.
[20] S. Huang, X. Wu, G. M. Cavalheiro, X. Du, B. Liu, Z. Du, G. Zhang, *J. Electrochem. Soc.* **2019**, *166*, A3254.
[21] T. Waldmann, B. I. Hogg, M. Wohlfahrt-Mehrens, *J. Power Sources* **2018**, *384*, 107.
[22] Z. M. Konz, Z. M. Konz, E. J. McShane, E. J. McShane, B. D. McCloskey, B. D. McCloskey, *ACS Energy Lett.* **2020**, *5*, 1750.
[23] E. J. McShane, E. J. McShane, A. M. Colclasure, D. E. Brown, D. E. Brown, Z. M. Konz, Z. M. Konz, K. Smith, B. D. McCloskey, B. D. McCloskey, *ACS Energy Lett.* **2020**, *5*, 2045.
[24] https://ec.europa.eu/growth/sectors/raw-materials/areas-specific-interest/critical-raw-materials_en (accessed: December 2022).
[25] X. Zhang, D. Wang, X. Qiu, Y. Ma, D. Kong, K. Müllen, X. Li, L. Zhi, *Nat. Commun.* **2020**, *11*, 3826.
[26] P. U. Nzereogu, A. D. Omah, F. I. Ezema, E. I. Iwuoha, A. C. Nwanya, *Appl. Surf. Sci. Adv.* **2022**, *9*, 100233.
[27] C. K. Chan, H. Peng, G. Liu, K. McIlwrath, X. F. Zhang, R. A. Huggins, Y. Cui, *Nat. Nanotechnol.* **2008**, *3*, 31.
[28] J. Graetz, C. C. Ahn, R. Yazami, B. Fultz, *Electrochem. Solid-State Lett.* **2003**, *6*, A194.
[29] U. Kasavajjula, C. Wang, A. J. Appleby, *J. Power Sources* **2007**, *163*, 1003.
[30] B. Gao, S. Sinha, L. Fleming, O. Zhou, *Adv. Mater.* **2001**, *13*, 819.
[31] M. Wachtler, M. Winter, J. O. Besenhard, *J. Power Sources* **2002**, *105*, 151.
[32] C. Zhang, F. Wang, J. Han, S. Bai, J. Tan, J. Liu, F. Li, *Small Struct.* **2021**, *2*, 2100009.
[33] D. Lin, Y. Liu, Y. Cui, *Nat. Nanotechnol.* **2017**, *12*, 194.
[34] L. Xiao, X. Chen, R. Cao, J. Qian, H. Xiang, J. Zheng, J. G. Zhang, W. Xu, *J. Power Sources* **2015**, *293*, 1062.
[35] X. Q. Zhang, X. B. Cheng, X. Chen, C. Yan, Q. Zhang, *Adv. Funct. Mater.* **2017**, *27*, 1605989.
[36] X. B. Cheng, C. Yan, X. Chen, C. Guan, J. Q. Huang, H. J. Peng, R. Zhang, S. T. Yang, Q. Zhang, *Chem* **2017**, *2*, 258.
[37] H. J. Peng, J. Q. Huang, X. B. Cheng, Q. Zhang, *Adv. Energy Mater.* **2017**, *7*, 1700260.
[38] D. Geng, N. Ding, T. S. A. Hor, S. W. Chien, Z. Liu, D. Wuu, X. Sun, Y. Zong, *Adv. Energy Mater.* **2016**, *6*, 1502164.
[39] S. Xia, X. Wu, Z. Zhang, Y. Cui, W. Liu, *Chem* **2019**, *5*, 753.
[40] J. Janek, W. G. Zeier, *Nat. Energy* **2016**, *1*, 16141.
[41] Y. K. Sun, *ACS Energy Lett.* **2020**, *5*, 3221.
[42] A. Masias, J. Marcicki, W. A. Paxton, *ACS Energy Lett.* **2021**, *6*, 621.
[43] M. Winter, B. Barnett, K. Xu, *Chem. Rev.* **2018**, *118*, 11433.
[44] https://electricautonomy.ca/2020/09/18/moli-energy-lithium-battery-technology/ (accessed: December 2022).
[45] X. Zhang, Y. Yang, Z. Zhou, *Chem. Soc. Rev.* **2020**, *49*, 3040.
[46] F. Wu, J. Maier, Y. Yu, *Chem. Soc. Rev.* **2020**, *49*, 1569.
[47] Q. Wang, B. Liu, Y. Shen, J. Wu, Z. Zhao, C. Zhong, W. Hu, *Adv. Sci.* **2021**, *8*, 2101111.
[48] W. Cao, Q. Li, X. Yu, H. Li, *eScience* **2022**, *2*, 47.
[49] X. Q. Zhang, X. B. Cheng, Q. Zhang, *Adv. Mater. Interfaces* **2018**, *5*, 1701097.
[50] Z. Luo, X. Qiu, C. Liu, S. Li, C. Wang, G. Zou, H. Hou, X. Ji, *Nano Energy* **2021**, *79*, 105507.
[51] Y. Zhang, T. T. Zuo, J. Popovic, K. Lim, Y. X. Yin, J. Maier, Y. G. Guo, *Mater. Today* **2020**, *33*, 56.
[52] C. Z. Zhao, H. Duan, J. Q. Huang, J. Zhang, Q. Zhang, Y. G. Guo, L. J. Wan, *Sci. China: Chem.* **2019**, *62*, 1286.
[53] S. Liu, W. Zhang, *Green Energy Environ.* **2021**, *6*, 791.
[54] B. Horstmann, J. Shi, R. Amine, M. Werres, X. He, H. Jia, F. Hausen, I. Cekic-Laskovic, S. Wiemers-Meyer, J. Lopez, D. Galvez-Aranda, F. Baakes, D. Bresser, C.-C. Su, Y. Xu, W. Xu, P. Jakes, R.-A. Eichel, E. Figgemeier, U. Krewer, J. M. Seminario, P. B. Balbuena, C. Wang, S. Passerini, Y. Shao-Horn, M. Winter, K. Amine, R. Kostecki, A. Latz, *Energy Environ. Sci.* **2021**, *14*, 5289.
[55] P. W. Gruber, P. A. Medina, G. A. Keoleian, S. E. Kesler, M. P. Everson, T. J. Wallington, *J. Indust. Ecol.* **2011**, *15*, 760.
[56] L. Talens Peiró, G. Villalba Méndez, R. U. Ayres, *JOM* **2013**, *65*, 986.
[57] W. H. Kruesi, D. J. Fray, *Metall. Trans. B* **1993**, *24*, 605.
[58] P. M. Brown, S. R. Jacob, *US4274834A*, **1979**.
[59] D. H. DeYoung, *US4988417A*, **1991**.
[60] A. Adachi, Y. Katayama, T. Miura, T. Kishi, *J. Power Sources* **1997**, *68*, 348.
[61] A. S. Basin, A. B. Kaplun, A. B. Meshalkin, N. F. Uvarov, *Russ. J. Inorg. Chem.* **2008**, *53*, 1509.
[62] H. Yu, G. Naidu, C. Zhang, C. Wang, A. Razmjou, D. S. Han, T. He, H. Shon, *Desalination* **2022**, *539*, 115951.
[63] A. Siekierka, M. Bryjak, A. Razmjou, W. Kujawski, A. N. Nikoloski, L. F. Dumée, *Membranes* **2022**, *12*, 343.
[64] a) H. Sinn, F. Sette, U. Bergmann, C. Halcoussis, M. Krisch, R. Verbeni, E. Burkel, *Phys. Rev. Lett.* **1997**, *78*, 1715; b) A. M. J. Schaeffer, W. B. Talmadge, S. R. Temple, S. Deemyad, *Phys. Rev. Lett.* **2012**, *109*, 185702.
[65] X. Zhang, A. Han, Y. Yang, *R. Soc. Chem.* **2020**, *8*, 22455.
[66] S. Yang, F. Zhang, H. Ding, P. He, H. Zhou, *Joule* **2018**, *2*, 1648.
[67] C. Liu, Y. Li, D. Lin, P. C. Hsu, B. Liu, G. Yan, T. Wu, Y. Cui, S. Chu, *Joule* **2020**, *4*, 1459.
[68] Z. Tang, X. Guan, *J. Sustainable Metall.* **2021**, *7*, 203.
[69] B. Zhang, H. Zhang, B. Ai, K. Pan, W. Zhang, D. Li, L. Zhang, Z. Shi, *ACS Appl. Eng. Mater.* **2022**, *1*, 59.
[70] E. Bodoin, L. Swonger, O. Mashtalir, S. O'Brien, *WO2017/095989A1*, **2017**.
[71] H. C. Meyer, *Adv. Chem.* **1957**, *19*, 9.
[72] F. Duffner, N. Kronemeyer, J. Tübke, J. Leker, M. Winter, R. Schmuch, *Nat. Res.* **2021**, *6*, 123.
[73] R. R. Yadav, Y. Dewang, J. Raghuvanshi, *Int. J. LNCT* **2018**, *2*, 124.
[74] J. J. Lewandowski, A. Awadallah, *ASM Handbook* **2005**, *14A*, 440.
[75] R. Laliberté, J. Dubé, *US7194884*, **2007**.
[76] R. Laliberté, J. Dube, *CA2768057C*, **2016**.
[77] L. Guo, H. Yang, *Compr. Mater. Process.* **2014**, *5*, 291.
[78] R. Schmuch, R. Wagner, G. Hörpel, T. Placke, M. Winter, *Nat. Energy* **2018**, *3*, 267.
[79] B. K. Hovsepian, *US3721113A*, **1971**.
[80] M. Gauthier, P. Bouchard, P.-E. Guerin, M. Armand, *EP0692669A1*, **1994**.
[81] P. Bouchard, P.-E. Guerin, G. St-Amant, G. Laroche, *EP0692831A1*, **1999**.
[82] T. H. Westmore, H. B. Eitouni, A. Nuval, R. C. Pratt, *US20190280292A1*, **2019**.
[83] Y. Xiaoxia, D. Jianping, Y. Zheng, W. Yulong, F. Hui, *CN106784600A*, **2016**.
[84] M. Wan, S. Kang, L. Wang, H. W. Lee, G. W. Zheng, Y. Cui, Y. Sun, *Nat. Commun.* **2020**, *11*, 829.
[85] P. Bouchard, P.-E. Guerin, G. St-Amant, G. Laroche, *US5528920A*, **1994**.
[86] J. Schnell, T. Günther, T. Knoche, C. Vieider, L. Köhler, A. Just, M. Keller, S. Passerini, G. Reinhart, *J. Power Sources* **2018**, *382*, 160.
[87] E. Ö. Jónsson, F. Larsson, *M.Sc. Thesis*, Chalmers University of Technology **2016**.

[88] B. Stumper, J. Dhom, L. Schlosser, D. Schreiner, A. Mayr, R. Daub, *Procedia CIRP* **2022**, *107*, 984.

[89] F. She, A. Gao, P. Jiang, Y. Zhou, X. Zhang, M. Yang, L. Gong, J. Chen, X. Lu, F. Xie, (Preprint), SSRN, https://ssrn.com/abstract=4285882, Submitted Nov; **2022**.

[90] P. M. Nogales, H.-Y. Song, M.-H. Jo, S.-K. Jeong, *Energies* **2022**, *15*, 1419.

[91] J. Becking, A. Gröbmeyer, M. Kolek, U. Rodehorst, S. Schulze, M. Winter, P. Bieker, M. C. Stan, *Adv. Mater. Interfaces* **2017**, *4*, 1700166.

[92] M. L. Meyerson, J. K. Sheavly, A. Dolocan, M. P. Griffin, A. H. Pandit, R. Rodriguez, R. M. Stephens, D. A. Vanden Bout, A. Heller, C. B. Mullins, *J. Mater. Chem. A* **2019**, *7*, 14882.

[93] H. Wang, Z.-L. Yi, F.-Y. Su, G. Song, L.-J. Xie, Z.-B. Wang, C.-M. Chen, *J. Power Sources* **2022**, *520*, 230817.

[94] N. Delaporte, Y. Wang, K. Zaghib, *Front. Mater.* **2019**, *6*, 267.

[95] X. Hu, Y. Gao, B. Zhang, L. Shi, Q. Li, *EcoMat.* **2022**, *4*, e12264.

[96] M. C. Morant-Miñana, G. Liendo, M. Cabello, A. Quintela, J. Blanco, S. Martin-Fuentes, M. Armand, L. Otaegui, A. Villaverde, *Energy Technol.* **2021**, *9*, 2100479.

[97] M. C. Morant-Miñana, L. Fernandez-Diaz, G. Liendo, J. Blanco, S. Martin-Fuentes, M. Armand, L. Otaegui, A. Villaverde, *J. Power Sources* **2023**, *555*, 232372.

[98] J. Castillo, A. Santiago, X. Judez, I. Garbayo, J. A. Coca Clemente, M. C. Morant – Miñana, A. Villaverde, J. A. González-Marcos, H. Zhang, M. Armand, C. Li, *Chem. Mater.* **2021**, *33*, 8812.

[99] J. Zagórski, B. Silván, D. Saurel, F. Aguesse, A. Llordés, *ACS Appl. Energy Mater.* **2020**, *3*, 8344.

[100] https://www.electrive.com/2021/03/03/actually-we-are-the-pioneer-of-solid-state-battery (accessed: December 2022).

[101] M. N. Rahaman, *Ceramic Processing and Sintering*, 2nd ed., Marcel Dekker, Inc., New York **2003**.

[102] T. Nishinaga, *Handbook of Crystal Growth: Thin Films and Epitaxy*, Elsevier Science, Amsterdam, The Netherlands **2014**.

[103] D. H. A. Blank, M. Dekkers, G. Rijnders, *J. Phys. D Appl. Phys.* **2013**, *47*, 034006.

[104] B. S. Vasile, A. C. Birca, V. A. Surdu, I. A. Neacsu, A. I. Nicoară, *Nanomaterials* **2020**, *10*, 370.

[105] U. Schulz, B. Saruhan, K. Fritscher, C. Leyens, *Int. J. Appl. Ceram. Technol.* **2004**, *1*, 302.

[106] J. G. Connell, T. Fuchs, H. Hartmann, T. Krauskopf, Y. Zhu, J. Sann, R. Garcia-Mendez, J. Sakamoto, S. Tepavcevic, J. Janek, *Chem. Mater.* **2020**, *32*, 10207.

[107] P. Liu, M. J. Counihan, Y. Zhu, J. G. Connell, D. Sharon, S. N. Patel, P. C. Redfern, P. Zapol, N. M. Markovic, P. F. Nealey, L. A. Curtiss, S. Tepavcevic, *Adv. Energy Sustainability Res.* **2022**, *3*, 2100142.

[108] I. Ruiz de Larramendi, N. Ortiz, R. López-Antón, J. I. R. de Larramendi, T. Rojo, *J. Power Sources* **2007**, *171*, 747.

[109] V. Palomares, I. Ruiz de Larramendi, J. Alonso, M. Bengoechea, A. Goñi, O. Miguel, T. Rojo, *Appl. Surf. Sci.* **2010**, *256*, 2563.

[110] C. M. Julien, A. Mauger, *Coatings* **2019**, *9*, 386.

[111] H. U. Krebs, O. Bremert, *Appl. Phys. Lett.* **1998**, *62*, 2341.

[112] I. Álvarez-Serrano, I. R. de Larramendi, M. L. López, C. Pico, T. Rojo, M. L. Veiga, *J. Alloys Compd.* **2011**, *509*, 1457.

[113] I. Álvarez-Serrano, I. Ruiz de Larramendi, M. L. López, M. L. Veiga, *Appl. Surf. Sci.* **2017**, *399*, 387.

[114] M. Fenech, N. Sharma, *Chem. Asian J.* **2020**, *15*, 1829.

[115] L. Indrizzi, N. Ohannessian, D. Pergolesi, T. Lippert, E. Gilardi, *Helv. Chim. Acta* **2021**, *104*, 2000203.

[116] W. Dong, K. Wang, J. Han, Y. Yu, G. Liu, C. Li, P. Tong, W. Li, C. Yang, Z. Lu, *ACS Appl. Mater. Interfaces* **2021**, *13*, 8417.

[117] J. Yi, J. Chen, Z. Yang, Y. Dai, W. Li, J. Cui, F. Ciucci, Z. Lu, C. Yang, *Adv. Energy Mater.* **2019**, *9*, 1901796.

[118] J. Kriegler, L. Hille, S. Stock, L. Kraft, J. Hagemeister, J. B. Habedank, A. Jossen, M. F. Zaeh, *Appl. Energy* **2021**, *303*, 117693.

[119] L. Gireaud, S. Grugeon, S. Laruelle, B. Yrieix, J. M. Tarascon, *Electrochem. Commun.* **2006**, *8*, 1639.

[120] K. Wasa, I. Kanno, H. Kotera, *Handbook of Sputter Deposition Technology: Fundamentals and Applications for Functional Thin Films*, 2nd ed., *Nano-Materials and MEMS*, Elsevier, UK **2012**.

[121] J. S. Chapin, *US4166018A*, **1974**.

[122] P. J. Kelly, R. D. Arnell, *Vacuum* **2000**, *56*, 159.

[123] D. L. Smith, *Thin-Film Deposition: Principles and Practice*, McGraw Hill Professional, New York **1995**.

[124] K. Seshan, *Handbook of Thin-Film Deposition Processes and Techniques*, Noyes Publication, New York **2002**.

[125] L. Fallarino, C. Binek, A. Berger, *Phys. Rev. B* **2015**, *91*, 214403.

[126] L. Fallarino, A. Oelschlägel, J. A. Arregi, A. Bashkatov, F. Samad, B. Böhm, K. Chesnel, O. Hellwig, *Phys. Rev. B* **2019**, *99*, 024431.

[127] L. Fallarino, B. J. Kirby, E. E. Fullerton, *J. Phys. D. Appl. Phys.* **2021**, *54*, 303002.

[128] S. M. Rossnagel, *IBM J. Res. Dev.* **1999**, *43*, 163.

[129] J. B. Bates, N. J. Dudney, G. R. Gruzalski, R. A. Zuhr, A. Choudhury, C. F. Luck, J. D. Robertson, *J. Power Sources* **1993**, *43*, 103.

[130] F. Wu, G. Tan, J. Lu, R. Chen, L. Li, K. Amine, *Nano Lett.* **2014**, *14*, 1281.

[131] Y. Chung, H. Y. Park, S. H. Oh, D. Y. Yoon, S. W. Jin, D. Y. Jang, J. M. Ko, W. Il Cho, S. R. Lee, *J. Electroceram.* **2013**, *31*, 316.

[132] K. Sivajee Ganesh, B. Purusottam Reddy, P. Jeevan Kumar, K. Jayanthbabu, P. Rosaiah, O. M. Hussain, *J. Solid State Electrochem.* **2015**, *19*, 3621.

[133] Y. Su, J. Falgenhauer, A. Polity, T. Leichtweiß, A. Kronenberger, J. Obel, S. Zhou, D. Schlettwein, J. Janek, B. K. Meyer, *Solid State Ionics* **2015**, *282*, 63.

[134] L. Li, X. Xue, S. Liu, H. Zhou, *Ionics* **2017**, *23*, 1451.

[135] T. Mousavi, X. Chen, C. Doerrer, B. Jagger, S. C. Speller, C. R. M. Grovenor, *Solid State Ionics* **2020**, *354*, 115397.

[136] C. S. Nimisha, K. Y. Rao, G. Venkatesh, G. M. Rao, N. Munichandraiah, *Thin Solid Films* **2011**, *519*, 3401.

[137] K. Wen, L. Liu, S. Chen, S. Zhang, *RSC Adv.* **2018**, *8*, 13034.

[138] K. Peng, B. Wang, Y. Li, C. Ji, *RSC Adv.* **2015**, *5*, 81468.

[139] T. Lee, W. K. Kim, Y. Lee, M. H. Ryou, Y. M. Lee, *Macromol. Res.* **2014**, *22*, 1190.

[140] J. Zhang, H. Q. Li, Q. Tang, P. W. Bai, Y. Y. Pan, Z. W. Lin, *RSC Adv.* **2016**, *6*, 114447.

[141] J. Li, Y. Jiang, F. Qin, J. Fang, K. Zhang, Y. Lai, *J. Electroanal. Chem.* **2018**, *823*, 537.

[142] J. Zhang, H. Li, Z. Lin, Q. Tang, W. Qi, L. Wang, H. Zheng, K. Zhou, *RSC Adv.* **2017**, *7*, 39172.

[143] X. Dai, A. Zhou, J. Xu, Y. Lu, L. Wang, C. Fan, J. Li, *J. Phys. Chem. C* **2016**, *120*, 422.

[144] D. Kang, M. Xiao, J. P. Lemmon, *Batteries Supercaps* **2021**, *4*, 445.

[145] L. Fan, H. L. Zhuang, L. Gao, Y. Lu, L. A. Archer, *J. Mater. Chem. A* **2017**, *5*, 3483.

[146] C. Rigaux, R. Vigneron, F. Bodart, Y. Jongen, A. Cambriani, S. Lucas, *Nucl. Instrum. Methods Phys. Res., Sect. B* **2008**, *266*, 2446.

[147] C. Rigaux, A. Lafort, F. Bodart, Y. Jongen, A. Cambriani, S. Lucas, *Plasma Processes Polym.* **2009**, *6*, S337.

[148] M. J. Neumann, D. Mehtani, S. Kailasam, T. Frank, T. Martin, J. Satern, Q. A. Song Nguyen, D. Shrivastava, A. A. Pradhan, R. T. Rozbicki, *US20140138242A1* **2012**.

[149] S. E. Mochalov, A. R. Nurgaliev, E. V. Kuzmina, A. L. Ivanov, V. S. Kolosnitsyn, *Vacuum* **2019**, *168*, 108816.

[150] K. S. Sree Harsha, *Principles of Physical Vapor Deposition of Thin Films*, Elsevier, New York **2006**.

[151] J. B. Bates, N. J. Dudney, B. Neudecker, A. Ueda, C. D. Evans, *Solid State Ionics* **2000**, *135*, 33.

[152] Y. Matsuda, N. Kuwata, J. Kawamura, *Solid State Ionics* **2018**, *320*, 38.

[153] B. J. Neudecker, N. J. Dudney, J. B. Bates, *J. Electrochem. Soc.* **2000**, *147*, 517.

[154] S. Tintignac, R. Baddour-Hadjean, J. P. Pereira-Ramos, R. Salot, *Electrochim. Acta* **2014**, *146*, 472.

[155] C. Li, W. Liu, Z. Fu, *Chin. J. Chem. Phys.* **2013**, *19*, 493.

[156] C. Navone, S. Tintignac, J. P. Pereira-Ramos, R. Baddour-Hadjean, R. Salot, *Solid State Ionics* **2011**, *192*, 343.

[157] N. Kuwata, N. Iwagami, Y. Tanji, Y. Matsuda, J. Kawamura, *J. Electrochem. Soc.* **2010**, *157*, A521.

[158] E. Cha, J. H. Yun, R. Ponraj, D. K. Kim, *Mater. Chem. Front.* **2021**, *5*, 6294.

[159] C.-C. Li, X.-S. Zhang, Y.-H. Zhu, Y. Zhang, S. Xin, L.-J. Wan, Y.-G. G. Li, *Energy Mater.* **2021**, *1*, 100017.

[160] S. H. Wang, J. Yue, W. Dong, T.-T. Zuo, J.-Y. Li, X. Liu, X.-D. Zhang, L. Liu, J.-L. Shi, Y.-X. Yin, Y.-G. Guo, *Nat. Commun.* **2019**, *10*, 4930.

[161] R. N. Wenzel, *Ind. Eng. Chem.* **1936**, *28*, 988.

[162] D. Quéré, *Annu. Rev. Mater. Res.* **2008**, *38*, 71.

[163] Z. Liang, D. Lin, J. Zhao, Z. Lu, Y. Liu, C. Liu, Y. Lu, H. Wang, K. Yan, X. Tao, Y. Cui, *Proc. Natl. Acad. Sci. USA* **2016**, *113*, 2862.

[164] G. French, *EP0357859A1*, **1988**.

[165] A. Sharafi, H. M. Meyer, J. Nanda, J. Wolfenstine, J. Sakamoto, *J. Power Sources* **2016**, *302*, 135.

[166] E. Kazyak, M. Shin, W. S. Lepage, T. H. Cho, N. P. Dasgupta, *Chem. Commun.* **2020**, *56*, 15537.

[167] R. V. Salvatierra, W. Chen, J. M. Tour, *Adv. Energy Sustainability Res.* **2021**, *2*, 2000110.

[168] K. Schönherr, B. Schumm, F. Hippauf, R. Lissy, H. Althues, C. Leyens, S. Kaskel, *Chem. Eng. J. Adv.* **2022**, *9*, 100218.

[169] Y. Chen, J. Li, Z. Lei, Y. Huo, L. Yang, S. Zeng, H. Ding, Y. Qin, Y. Jie, F. Huang, Q. Li, J. Zhu, R. Cao, G. Zhang, S. Jiao, D. Xu, *Adv. Energy Mater.* **2020**, *10*, 1903401.

[170] J.-F. Ding, Y.-T. Zhang, R. Xu, R. Zhang, Y. Xiao, S. Zhang, C.-X. Bi, C. Tang, R. Xiang, H. S. Park, Q. Zhang, J.-Q. Huang, *Green Energy Environ.*, in press **2022**.

[171] B. Li, J. Xu, X. Xiao, *Langmuir* **2019**, *35*, 16459.

[172] X. B. Cheng, T. Z. Hou, R. Zhang, H. J. Peng, C. Z. Zhao, J. Q. Huang, Q. Zhang, *Adv. Mater.* **2016**, *28*, 2888.

[173] X. Shen, Y. Li, T. Qian, J. Liu, J. Zhou, C. Yan, J. B. Goodenough, *Nat. Commun.* **2019**, *10*, 900.

[174] R. Laliberte, P. Sirois, R. Gagnon, *US7513136B2*, **2003**.

[175] M. Yakovleva, K. B. Fitch, J. Xia, W. A. Greeter, *US20220149341A1,* **2019**.

[176] J. Xia, B. Fitch, A. Watson, E. Cabaniss, R. Black, M. Yakovleva, *ECS Meeting Abstracts* **2020**, *MA2020-02*, 976.

[177] G. Zangari, *Fundamentals of Electrodeposition*, Elsevier, New York **2018**, p. 141.

[178] K. Kanamura, S. Shiraishi, Z. Takehara, *J. Electrochem. Soc.* **1994**, *141*, L108.

[179] S. Shiraishi, K. Kanamura, Z. Takehara, *J. Electrochem. Soc.* **1999**, *146*, 1633.

[180] J. Qian, W. Xu, P. Bhattacharya, M. Engelhard, W. A. Henderson, Y. Zhang, J. G. Zhang, *Nano Energy* **2015**, *15*, 135.

[181] K. Yoshii, H. Kiuchi, N. Taguchi, M. Shikano, E. Matsubara, H. Sakaebe, *ChemElectroChem* **2020**, *7*, 4336.

[182] H. Koshikawa, S. Matsuda, K. Kamiya, Y. Kubo, K. Uosaki, K. Hashimoto, S. Nakanishi, *J. Power Sources* **2017**, *350*, 73.

[183] J. Liu, Z. Bao, Y. Cui, E. J. Dufek, J. B. Goodenough, P. Khalifah, Q. Li, B. Y. Liaw, P. Liu, A. Manthiram, Y. S. Meng, V. R. Subramanian, M. F. Toney, V. V. Viswanathan, M. S. Whittingham, J. Xiao, W. Xu, J. Yang, X.-Q. Yang, J.-G. Zhang, *Nat. Energy* **2019**, *4*, 180.

[184] Y. Liu, D. Lin, Y. Li, G. Chen, A. Pei, O. Nix, Y. Li, Y. Cui, *Nat. Commun.* **2018**, *9*, 3656.

[185] F. Ding, W. Xu, G. L. Graff, J. Zhang, M. L. Sushko, X. Chen, Y. Shao, M. H. Engelhard, Z. Nie, J. Xiao, X. Liu, P. V. Sushko, J. Liu, J.-G. Zhang, *J. Am. Chem. Soc.* **2013**, *135*, 4450.

[186] O. Mashtalir, M. Nguyen, E. Bodoin, L. Swonger, S. P. O'Brien, *ACS Omega* **2018**, *3*, 181.

[187] H. Porthault, C. Decaux, *Electrochim. Acta* **2016**, *194*, 330.

[188] W. Plieth, *Electrochemistry for Materials Science*, Elsevier, New York **2008**.

[189] O. B. Chae, J. Kim, B. L. Lucht, *J. Power Sources* **2022**, *532*, 231338.

[190] L. R. Swonger, N. K. Karan, *US20210269930A1*, **2019**.

[191] L. R. Swonger, E. Bodoin, *US10177366B2*, **2020**.

[192] L. R. Swonger, *US20220010447A1*, **2019**.

[193] T. Matsui, K. Takeyama, *JP3202880B2*, **1994**.

[194] J. H. Kim, H.-Y. Bae, M. K. Cho, N. S. Choi, S.-L. Lee, W.-S. Bae, Y. W. Lee, J.-W. Moon, *US20190348668A1*, **2017**.

[195] Y. Gu, H. Y. Xu, X. G. Zhang, W. W. Wang, J. W. He, S. Tang, J. W. Yan, D. Y. Wu, M. Sen Zheng, Q. F. Dong, B. W. Mao, *Angew. Chem., Int. Ed.* **2019**, *58*, 3092.

[196] Y. J. Kim, S. H. Kwon, H. Noh, S. Yuk, H. Lee, H. S. Jin, J. Lee, J. G. Zhang, S. G. Lee, H. Guim, H. T. Kim, *Energy Storage Mater.* **2019**, *19*, 154.

[197] J. Y. Kim, O. B. Chae, M. Wu, E. Lim, G. Kim, Y. J. Hong, W. Bin Jung, S. Choi, D. Y. Kim, I. Gereige, J. Suk, Y. Kang, H. T. Jung, *Nano Energy* **2021**, *82*, 105736.

[198] C. Shen, J. Gu, N. Li, Z. Peng, K. Xie, *J. Power Sources* **2021**, *501*, 229969.

[199] S. S. Zhang, X. Fan, C. Wang, *Electrochem. Commun.* **2018**, *89*, 23.

[200] C. J. Huang, Y. C. Hsu, K. N. Shitaw, Y. J. Siao, S. H. Wu, C. H. Wang, W. N. Su, B. J. Hwang, *ACS Appl. Mater. Interfaces* **2022**, *14*, 26724.

[201] S. Liu, X. Zhang, R. Li, L. Gao, J. Luo, *Energy Storage Mater.* **2018**, *14*, 143.

[202] Q. Li, H. Pan, W. Li, Y. Wang, J. Wang, J. Zheng, X. Yu, H. Li, L. Chen, *ACS Energy Lett.* **2018**, *3*, 2259.

[203] Z. L. Zhang, Y. Jin, Y. Zhao, J. Xu, B. Sun, K. Liu, H. Lu, N. Lv, Z. Dang, H. Wu, *Nano Res.* **2021**, *14*, 3999.

[204] C. Chen, Y. Yang, H. Shao, *Electrochim. Acta* **2014**, *137*, 476.

[205] K. Yan, Z. Lu, H. W. Lee, F. Xiong, P. C. Hsu, Y. Li, J. Zhao, S. Chu, Y. Cui, *Nat. Energy* **2016**, *1*, 16010.

[206] H. Ye, Z.-J. Zheng, H.-R. Yao, S.-C. Liu, T.-T. Zuo, X.-W. Wu, Y.-X. Yin, N.-W. Li, J.-J. Gu, F.-F. Cao, Y.-G. Guo, *Angew. Chem.* **2019**, *131*, 1106.

[207] B. Ji, F. Zhang, M. Sheng, X. Tong, Y. Tang, *Adv. Mater.* **2017**, *29*, 1604219.

[208] C. Wu, H. Huang, W. Lu, Z. Wei, X. Ni, F. Sun, P. Qing, Z. Liu, J. Ma, W. Wei, L. Chen, C. Yan, L. Mai, *Adv. Sci.* **2020**, *7*, 1902643.

[209] S. S. Zhang, X. Fan, C. Wang, *Electrochim. Acta* **2017**, *258*, 1201.

[210] Y. Ma, L. Wang, S. Fu, R. Luo, W. Qu, X. Hu, R. Chen, F. Wu, L. Li, *J. Mater. Chem. A* **2020**, *8*, 23574.

[211] T. Liu, Q. Hu, X. Li, L. Tan, G. Yan, Z. Wang, H. Guo, Y. Liu, Y. Wu, J. Wang, *J. Mater. Chem. A* **2019**, *7*, 20911.

[212] S. Cui, P. Zhai, W. Yang, Y. Wei, J. Xiao, L. Deng, Y. Gong, *Small* **2020**, *16*, 1905620.

[213] Y. G. Lee, S. Fujiki, C. Jung, N. Suzuki, N. Yashiro, R. Omoda, D. S. Ko, T. Shiratsuchi, T. Sugimoto, S. Ryu, J. H. Ku, T. Watanabe, Y. Park, Y. Aihara, D. Im, I. T. Han, *Nature Energy* **2020**, *5*, 299.

[214] C. P. Yang, Y. X. Yin, S. F. Zhang, N. W. Li, Y. G. Guo, *Nat. Commun.* **2015**, *6*, 8058.

[215] L. L. Lu, J. Ge, J. N. Yang, S. M. Chen, H. Bin Yao, F. Zhou, S. H. Yu, *Nano Lett.* **2016**, *16*, 4431.

[216] Q. Yun, Y. B. He, W. Lv, Y. Zhao, B. Li, F. Kang, Q. H. Yang, *Adv. Mater.* **2016**, *28*, 6932.

[217] H. Zhao, D. Lei, Y. B. He, Y. Yuan, Q. Yun, B. Ni, W. Lv, B. Li, Q. H. Yang, F. Kang, J. Lu, *Adv. Energy Mater.* **2018**, *8*, 1800266.
[218] Y. Tang, K. Shen, Z. Lv, X. Xu, G. Hou, H. Cao, L. Wu, G. Zheng, Y. Deng, *J. Power Sources* **2018**, *403*, 82.
[219] H. N. Umh, J. Park, J. Yeo, S. Jung, I. Nam, J. Yi, *Electrochem. Commun.* **2019**, *99*, 27.
[220] J. Chen, J. Zhao, L. Lei, P. Li, J. Chen, Y. Zhang, Y. Wang, Y. Ma, D. Wang, *Nano Lett.* **2020**, *20*, 3403.
[221] S. H. Wang, Y. X. Yin, T. T. Zuo, W. Dong, J. Y. Li, J. L. Shi, C. H. Zhang, N. W. Li, C. J. Li, Y. G. Guo, *Adv. Mater.* **2017**, *29*, 1703729.
[222] K. H. Chen, A. J. Sanchez, E. Kazyak, A. L. Davis, N. P. Dasgupta, *Adv. Energy Mater.* **2019**, *9*, 1802534.
[223] P. Zou, Y. Wang, S. W. Chiang, X. Wang, F. Kang, C. Yang, *Nat. Commun.* **2018**, *9*, 464.
[224] X. He, Y. Yang, M. S. Cristian, J. Wang, X. Hou, B. Yan, J. Li, T. Zhang, E. Paillard, M. Swietoslawski, R. Kostecki, M. Winter, J. Li, *Nano Energy* **2020**, *67*, 104172.
[225] H. Liu, X. Yue, X. Xing, Q. Yan, J. Huang, V. Petrova, H. Zhou, P. Liu, *Energy Storage Mater.* **2019**, *16*, 505.
[226] W. Liu, D. Lin, A. Pei, Y. Cui, *J. Am. Chem. Soc.* **2016**, *138*, 15443.
[227] L. Fan, H. L. Zhuang, W. Zhang, Y. Fu, Z. Liao, Y. Lu, *Adv. Energy Mater.* **2018**, *8*, 1703360.
[228] W. Zhang, H. L. Zhuang, L. Fan, L. Gao, Y. Lu, *Sci. Adv.* **2018**, *4*, eaar4410.
[229] X. Li, Y. Li, Y. Tang, L. Zhang, J. Huang, *J. Power Sources* **2021**, *496*, 229868.
[230] J. Pu, J. Li, K. Zhang, T. Zhang, C. Li, H. Ma, J. Zhu, P. V. Braun, J. Lu, H. Zhang, *Nat. Commun.* **2019**, *10*, 1896.
[231] S. Kim, Y. Kim, C. T. Nguyen, T. Jang, H. B. R. Lee, H. R. Byon, *J. Power Sources* **2020**, *472*, 228495.
[232] S. Liu, A. Wang, Q. Li, J. Wu, K. Chiou, J. Huang, J. Luo, *Joule* **2018**, *2*, 184.
[233] J. Xie, J. Wang, H. R. Lee, K. Yan, Y. Li, F. Shi, W. Huang, A. Pei, G. Chen, R. Subbaraman, J. Christensen, Y. Cui, *Sci. Adv.* **2018**, *4*, 5168.
[234] C. Yang, Y. Yao, S. He, H. Xie, E. Hitz, L. Hu, *Adv. Mater.* **2017**, *29*, 1702714.
[235] P. Xue, S. Liu, X. Shi, C. Sun, C. Lai, Y. Zhou, D. Sui, Y. Chen, J. Liang, *Adv. Mater.* **2018**, *30*, 1804165.
[236] B. Hong, H. Fan, X. B. Cheng, X. Yan, S. Hong, Q. Dong, C. Gao, Z. Zhang, Y. Lai, Q. Zhang, *Energy Storage Mater.* **2019**, *16*, 259.
[237] T. T. Zuo, X. W. Wu, C. P. Yang, Y. X. Yin, H. Ye, N. W. Li, Y. G. Guo, *Adv. Mater.* **2017**, *29*, 1700389.
[238] H. Ye, S. Xin, Y. X. Yin, J. Y. Li, Y. G. Guo, L. J. Wan, *J. Am. Chem. Soc.* **2017**, *139*, 5916.
[239] R. A. Shaw, *Global lithium (Li) mines, deposits, and occurrences*, British Geological Survey **2021**.

Begoña Acebedo graduated in chemical sciences from the University of the Basque Country (UPV/EHU) in 2003. She has developed her research career at the UPV/EHU and in the last decade in CIC Energigune focused on energy storage systems and working as laboratory technician. Initially, she worked in developing cathodes for lithium and sodium ion batteries, as well as polymeric electrolytes. In the last years, as Ph.D. candidate, her main interest has been the development of anodes for lithium metal batteries.

Maria C. Morant-Miñana obtained her Ph.D. at the Universitat de València and after several postdoctoral stays in various European centres of excellence she joined to CIC energiGUNE in 2018. Currently, she is associate researcher in the device prototyping group working mainly in polymeric solid-state batteries based on lithium metal. Her work intends to transform and integrate innovative materials into electrodes with excellent electrochemical performance.

Elena Gonzalo received her Ph.D. in chemistry from Complutense University (UCM), Madrid (Spain) in 2011, on the study of Transition Metal Fluorides and Chlorides as electrodes for Lithium-ion batteries. During here Ph.D., she undertook research stays at Uppsala University (Sweden), University of Tubingen (Germany), and University of Bath (UK). First joining CIC energiGUNE in 2012 as a postdoctoral researcher, she was promoted to senior researcher in 2017. Currently her research interests are focused on new lithium- and sodium-based electrode materials for rechargeable batteries, and in studying the interphases between all cell components.

Idoia Ruiz de Larramendi is senior lecturer of inorganic chemistry at the University of the Basque Country (UPV/EHU). Her research activity is related to the interdisciplinary and multidisciplinary field of materials science, both as academic and technologically oriented work. Her main motivation is to unravel and understand the properties of materials through multitechnical approaches. She combines materials development with a wide range of characterization techniques to decipher the mechanisms behind the materials' performance. With a keen interest in sustainable development, she aspires to advance the field of energy storage with the goal of accelerating market adoption of low-carbon technologies.

Aitor Villaverde is the cell prototyping group leader at CIC energiGUNE. His expertise is device design and new process development in different energy applications and since 2013 singularly in battery technologies and very focused on Li metal anodes technologies in the last years. He is in charge of providing industrial transference of next generation batteries toward cleaner and reduced carbon footprint processes.

Jokin Rikarte is a senior researcher at CIC energiGUNE. His background is on battery materials, particularly on the study of surfaces and interphases in different battery technologies, such as Li-ion batteries or Li-S batteries. Currently, his research is focused on the development of stable metallic lithium electrodes for different battery technologies and advanced current collectors toward anodeless lithium batteries.

Lorenzo Fallarino is a senior researcher at CIC energiGUNE. He is an expert in the fabrication and characterization of advanced multifunctional (nano-)materials. Overall, his research aims to the basic understanding and development of new material concepts to achieve fully tunable magnetic, electric, chemical, and thermal effects. At present, he is focusing to create sustainable energy storage systems from environmentally friendly and available materials and processes. In addition, he has planned and coordinated neutron, X-rays, and ion-beam experiments.